VIBRATIONS OF A THREE-LAYER BEAM WITH A VISCOELASTIC MIDDLE LAYER

Thesis by

David Edwin Van Dillen

In Partial Fulfillment of the Requirements

For the Degree of

Aeronautical Engineer

California Institute of Technology

Pasadena, California

1972

(Submitted May 26, 1972)

ACKNOWLEDGEMENTS

I wish to express my gratitude to Dr. Charles D. Babcock, Jr. for recommending to me what turned out to be a satisfying course of study, and for advising me toward a successful conclusion. I am also grateful to Dr. Ernest E. Sechler for his suggestions regarding the experimental setup, and to Dr. Wolfgang G. Knauss for his contributions in characterizing the mechanical properties of Solithane 113. I very much appreciate the efforts of Liz Fox, for typing this thesis, and of Betty Wood, for drawing the graphs and figures. Finally, I thank my wife, Sylvia, for making it possible for me to spend the time necessary to complete this thesis.

This study was supported, in part, by the Air Force Office of Scientific Research, Office of Aerospace Research, United States Air Force under Grant No. AFOSR 68-1424.

ABSTRACT

The equations governing a three-layer beam in which the middle layer is viscoelastic were derived by means of a variational principle. These equations were solved subject to arbitrary time dependent boundary conditions of both the simply-supported and cantilever type. In the simply-supported case, an eigenfunction expansion was constructed after the governing equations had been transformed through operation by a differential operator. In the cantilever case, the solution was obtained by Fourier transform with respect to time, and inversion by residue theory. An analysis of the theoretical response of the cantilever beam to steady state sinusoidal loading was carried out, and an experiment was conducted for comparison.

TABLE OF CONTENTS

LIST OF FIGURES

LIST OF TABLES

NOMENCLATURE

a_j $(j = 1, 2, 3)$ Coefficients in homogeneous solutions (4.24) and (5.6).

a_T Time-temperature shift factor. p. 75 (A.7).

A Set of all kinematically admissible states. p. 77.

$A_{nm}(t)$ p. 43 (4.38).

b Width of beam.

b_j $(j = 1, 2, 3)$ Coefficients in homogeneous solutions (4.24) and (5.6).

B Surface of a body.

B_1 That portion of the surface on which displacement boundary conditions are prescribed.

B_2 That portion of the surface on which traction boundary conditions are prescribed.

$B_j [v(x, t), \varphi(x, t)]$ $(j = 1, 2, \ldots, 6)$

Boundary conditions: simply-supported, p. 26 (4.4); cantilever, p. 41 (5.1).

$\mathcal{B}$ Matrix resulting from application of boundary conditions. p. 83 (C.2).

c p. 34 (4.20).

c_{nm} Coefficients in eigenfunction expansion. p. 38 (4.30).

$C(\kappa), C_j(\kappa)$ $(j = 1, 2, 3)$

p. 86 (C.6).

$\underline{d}(\underline{x})$ Initial displacement field of a body. p. 77 (B.4).

d_n Coefficients in eigenfunction expansion. p. 38 (4.30).

D Differential operator. p. 10 (2.13).

NOMENCLATURE (Cont'd)

$E, E(t), \tilde{E}(\omega)$	Young's modulus, Young's relaxation modulus, Young's complex modulus.
E_o	Young's modulus of outer layers in symmetrical beam.
$E_1, E_2(t), E_3$	Young's moduli of layers 1, 2, 3 in asymmetric beam.
$\mathcal{E}$	Curve fitting error. p. 72 (A. 3).
$\underline{f}(\underline{x}, t)$	p. 77 (B. 6).
$\underline{F}(\underline{x}, t)$	Body force field.
$\mathcal{F}_t\{\varphi(t)\}$	Fourier transform. p. 5 (2. 5).
$g(t)$	p. 77 (B. 5).
$g_{vj}(x)$, $g_{\varphi j}(x)$ $(j = 1, 2, \ldots, 6)$	Simply-supported, p. 27 (4. 8); cantilever, p. 46 (5. 2).
$\underline{G}(\underline{x}, t)$	Anisotropic relaxation modulus tensor.
$G(\omega)$	p. 34 (4. 20).
G_m	A known value of the complex shear modulus at frequency $\tilde{\omega}_m$.
h	p. 34 (4. 20).
h_M, h_o	Thicknesses of middle and outer layers in symmetrical beam.
h_1, h_2, h_3	Thicknesses of layers 1, 2, 3 in asymmetric beam.
$H(t)$	Unit step function. p. 7.
$\mathcal{I}(z)$	Imaginary part of complex number z.
$K, K(t), \tilde{K}(\omega)$	Bulk modulus, bulk relaxation modulus, bulk complex modulus.

NOMENCLATURE (Cont'd)

L Length of beam.

$L_j[v(x,t), \varphi(x,t)]$ $(j = 1, 2)$ p. 25 (4.2).

$M_j(x,t)$ $(j = 1, 2, 3)$ Resultant moment on layer j. p. 89 (Fig. 3).

$\underline{n}(\underline{x})$ Unit outward normal vector of surface B.

N Number of terms in exponential series representation of complex modulus.

$N_j(x,t)$ $(j = 1, 2, 3)$ Resultant axial force on layer j. p. 89 (Fig. 3).

$p(x,t)$ Transverse load applied to beam. p. 89 (Fig. 3).

$P_j(x,t)$ $(j = 1, 2)$ p. 28 (4.9).

$q_j(t)$ $(j = 1, 2, \ldots, 6)$ Prescribed values of boundary conditions at ends of beam.

$Q(x,t)$ Resultant shear force on beam cross-section.

R Region of space occupied by a body.

$\mathcal{R}(z)$ Real part of complex number z.

$\underline{\mathring{s}}(\underline{x},t)$ Prescribed value of traction boundary conditions.

S State. p. 77.

t Time

T Temperature in degrees, centigrade.

$T(t,\kappa)$ p. 86 (C.7).

$u(x,t)$ p. 31 (4.13), (4.14).

$\underline{u}(\underline{x},t)$ Displacement vector.

NOMENCLATURE (Cont'd)

$\underline{\mathring{u}}(\underline{x}, t)$	Prescribed value of displacement boundary conditions.
$\tilde{u}(x, t)$	Displacement in x direction of point x on the reference axis. p. 88 (Fig. 2).
$\underset{\sim}{\tilde{y}}(x)$, $\underset{\sim}{\mathring{\tilde{y}}}(x)$	Prescribed initial axial displacement and velocity of reference axis. p. 18 (3.5).
$\underset{\sim}{\mathring{y}}(x)$	p. 31 (4.14).
$\hat{u}_c(x, \kappa)$	p. 48 (5.6).
$\hat{u}_p(x, \kappa)$	p. 49 (5.7).
$U(x, \kappa)$	p. 85 (C.4).
$v(x, t)$	Displacement in the y direction of point x on the reference axis. p. 88 (Fig. 2).
$\underline{v}(\underline{x})$	Initial velocity field of a body. p. 77 (B.4).
$\underset{\sim}{y}(x)$, $\underset{\sim}{\mathring{y}}(x)$	Prescribed initial transverse displacement and velocity of reference axis. p. 18 (3.5).
$w(x, t)$	p. 27 (4.7).
$\underset{\sim}{w}(x)$, $\underset{\sim}{\mathring{w}}(x)$	p. 28 (4.11).
$W(x, \kappa)$	p. 85 (C.5).
x	Coordinate. p. 88 (Fig. 2).
$\underline{x}$	Position vector.
y	Coordinate. p. 88 (Fig. 2).
z, Z	p. 61.
$\underline{\alpha}$	p. 82 (C.1).
$\underline{\beta}$	p. 82 (C.1).
$\underline{\gamma}(\underline{x}, t)$	Strain tensor.
$\delta(t)$	Delta function.

NOMENCLATURE (Cont'd)

$\delta\Omega\{S\}$	Variation of the functional $\Omega\{S\}$. p. 78.
δ_{ij}	Component of Kronecker delta.
$\Delta(\kappa)$	Determinant of $\mathcal{B}$. p. 84 (C. 3).
$\Delta'(\kappa)$	p. 86 (C. 8).
$\epsilon_{jk\ell}$	Component of permutation tensor.
$\theta(x, t)$	p. 31 (4. 13), (4. 14).
$\hat{\theta}_c(x, \kappa)$	p. 48 (5. 6).
$\hat{\theta}_p(x, \kappa)$	p. 49 (5. 7).
$\circledH(x, \kappa)$	p. 85 (C. 4).
κ	Fourier transform parameter.
κ_j	jth iteration of eigenvalue. p. 58 (6. 4).
$\lambda_1, \lambda_2, \lambda_3$	Roots of (4. 23), p. 35.
$\mu, \mu(t), \tilde{\mu}(\omega)$	Shear modulus, shear relaxation modulus, shear complex modulus.
$\mu_2(t), \mu_M(t)$	Shear relaxation modulus of the middle layer.
μ_E, μ_k $(k = 1, 2, \ldots, N)$	Parameters in the exponential series representation of the shear relaxation modulus. p. 25 (4. 1).
$\tilde{\nu}(\omega)$	Complex Poisson's ratio.
ν_{nm}	p. 52.
ρ	p. 34 (4. 20).
$\rho(\underline{x})$	Density of a body.
ρ_M, ρ_o	Densities of middle and outer layers for symmetrical beam.

NOMENCLATURE (Cont'd)

ρ_1, ρ_2, ρ_3	Densities of layers 1, 2, 3 for asymmetric beam.
$\underline{\sigma}(\underline{x}, t)$	Stress tensor.
τ_k $(k = 1, 2, \ldots, N)$	Time constants in the exponential series representation of the complex modulus.
$\varphi(x, t)$	Rotation of the cross-section of the middle layer at point x of the reference axis. p. 88 (Fig. 2).
$\varphi(x), \dot{\varphi}(x)$	Prescribed initial rotation and angular velocity of the cross-section of the middle layer. p. 18 (3.5).
$\Phi\{S\}$	p. 78 (B.9).
$\psi(x, t)$	p. 27 (4.7).
$\Psi(x, \kappa)$	p. 85 (C.5).
ω	Frequency.
ω_n	p. 51.
ω_{nm}	Roots of (4.27), p. 37.
$\tilde{\omega}_m$	Frequency for which the complex shear modulus is known.

Other Notation:

a_i	Component of vector $\underline{a}$.
a_{ij}	Component of second order tensor or matrix.
$a_{,j}$	$\frac{\partial a}{\partial x_j}$
$\underline{a}$	Vector or tensor.
$\hat{a}(\kappa)$	Fourier transform of a(t). p. 5 (2.5).
$a'(x, t)$	$\frac{\partial}{\partial x} a(x, t)$
$\dot{a}(x, t)$	$\frac{\partial}{\partial t} a(x, t)$

NOMENCLATURE (Cont'd)

$\overline{a}$	Complex conjugate of a.
$a(t)*b(t)$	Riemann convolution. p. 30.
$a(t)*db(t)$	Stieltjes convolution. p. 30.
$[a(t)]^{-1}$	Stieltjes inverse. p. 8 (2.10).

1. Introduction

The problem considered in this paper is the dynamic response of a three-layer beam consisting of two identical elastic layers and a viscoelastic middle layer. Composite structural members containing viscoelastic layers are recognized as having desirable damping properties for many applications. Considerable attention, therefore, has been focussed on the accumulation of quantitative information concerning the response of such members to dynamic loads. Plass (ref. 1) analyzed the response of a viscoelastic sandwich beam to such elementary motions as pure bending and pure shear of the middle layer. Schwarzl (ref. 2) pointed out some of the complications which arise in the analysis of a two-layer viscoelastic beam in which the loss tangents of the two layers are different. Kerwin (ref. 3) and Ross, Ungar, and Kerwin (ref. 4) pointed out the superiority of the mechanism of shear damping over extensional damping. Yu (ref. 5) developed and analyzed a formulation of an infinite, symmetrical, three-layer viscoelastic plate in which there were no restrictions concerning the thickness ratio of the middle and outer layers. Di Taranto (ref. 6) considered a three-layer beam of finite length in which the cross section need not be symmetrical. The work of Nicholas (ref. 7) provided a timely check on the trend of the layered viscoelastic beam formulations to include the effects of shear deformations while neglecting the effects of rotatory inertia. Kovac, Anderson, and Scott (ref. 8) extended the analysis of viscoelastic sandwich beams to include non-linear effects.

All of these authors, with the exception of Plass (ref. 1) and Kovac, Anderson, and Scott (ref. 8), who represented the material behavior of the viscoelastic layer in terms of the most elementary spring and damper models, used the complex modulus characterization of the viscoelastic layer in order to analyze the steady state response of the beam to sinusoidal loading. Typical of the solution techniques employed by these authors is the application of what Bland (ref. 9, p. 67) quotes as the correspondence principle for sinusoidal oscillations. This method requires the corresponding elastic problem to be solved as completely as possible without using explicit numerical values for the elastic moduli. When the analysis of the corresponding elastic problem has come to a halt, either through completing the analysis or by encountering an operation too difficult to perform analytically, the elastic moduli are replaced by the values of the corresponding complex moduli for the value of the frequency of excitation under consideration. In the case of the simply-supported three-layer beam, this results in an analytic expression, in terms of an infinite series, for the solution of the viscoelastic steady state response problem. In more complicated cases, such as the cantilever, one can go no farther than to establish the characteristic frequency equation, the expressions for the eigenfunctions, and the orthogonality condition. Then the eigenvalues are found numerically; from these the eigenfunctions are obtained; and, using the orthogonality condition, the solution is constructed. This method suffers the limitation that, for the more complicated boundary conditions, the eigenvalues and eigenfunctions are dependent upon the given value of the

frequency of excitation. If one wishes to consider the response of the beam to a different frequency, a new set of eigenvalues and eigenfunctions must first be found. It is, therefore, computationally time consuming to undertake a study of the dependence of the response of the beam on the frequency of excitation, through application of this correspondence principle.

In order to find a more convenient form of the solution for the purpose of conducting a frequency response study, it was decided to avoid using the correspondence principle. It was possible, therefore, to consider not only steady state sinusoidal loading histories, but arbitrary loading histories. The characteristic frequency equation was obtained from the boundary-initial value problem governing the three-layer beam by application of a differential operator in the case of simply-supported boundary conditions, and by Fourier transform in the case of the cantilever. The resulting distributions of eigenvalues were more complicated than those which would have resulted from application of the correspondence principle, and no orthogonality condition involving the eigenfunctions of the cantilever was found. But the eigenvalues were independent of the loading history, and the Fourier transform procedure did not require an orthogonality condition for the construction of the solution. The resulting solutions, in addition to their capability of permitting a wide variety of loading conditions, were in a convenient form for the study of frequency response.

2. Constitutive Relations

For a linearly viscoelastic material, the relationship between the stress history and the strain history can be expressed by a hereditary integral of the form

$$\sigma(\underline{x}, t) = \gamma(\underline{x}, t) * d\, E(t) \qquad (2.1)$$

where $\sigma(\underline{x}, t)$ is the stress history at position $\underline{x}$, $\gamma(\underline{x}, t)$ is the strain history, and $E(t)$ is the relaxation modulus, a material property. Equation (2.1) can be thought of as describing a uniaxial stress state. Throughout this paper it is assumed that prior to time $t = 0$, the body under consideration is quiescent, i.e.,

$$\sigma(\underline{x}, t) = 0, \quad \gamma(\underline{x}, t) = 0 \quad (-\infty < t < 0)$$

Furthermore, it is a property of the relaxation modulus that

$$E(t) = 0 \qquad (-\infty < t < 0) \ .$$

The operation on the right-hand side of (2.1) is the Stieltjes convolution, defined as follows (ref. 10):

$$\varphi(t) * d\psi(t) = \int_{-\infty}^{t} \varphi(t-\tau) d\psi(\tau) \qquad (2.2)$$

where $\varphi(t)$ and $\psi(t)$ are functions defined for $0 \leq t < \infty$ and $-\infty < t < \infty$, respectively. Many useful identities involving Stieltjes convolutions are listed in ref. 10.

The complex modulus of a viscoelastic material is defined as the ratio of stress to strain in the case of sinusoidal motion, after the steady state has been achieved. Thus,

$$\sigma(\underline{x})\exp(i\omega t) = \tilde{E}(\omega)\gamma(\underline{x})\exp(i\omega t) \tag{2.3}$$

where $\tilde{E}(\omega)$ is the complex modulus, $\sigma(\underline{x})$ and $\gamma(\underline{x})$ are complex, and the frequency, ω, is real. Taking $\sigma(\underline{x}, t) = \sigma(\underline{x})\exp(i\omega t)$, and $\gamma(\underline{x}, t) = \gamma(\underline{x})\exp(i\omega t)$ in (2.1), one gets

$$\sigma(\underline{x})\exp(i\omega t) = \gamma(\underline{x})\exp(i\omega t)*dE(t)$$

$$\sigma(\underline{x})\exp(i\omega t) = \gamma(\underline{x})\exp(i\omega t)\left\{E(0)+\int_0^t \exp(-i\omega\tau)\,\dot{E}(\tau)d\tau\right\}$$

In order for the above equation to describe the steady state, ∞ must replace t as the upper limit of integration. Comparing this result with (2.3), one can write the complex modulus in terms of the relaxation modulus; thus,

$$\tilde{E}(\omega) = E(0) + \int_0^\infty \exp(-i\omega\tau)\dot{E}(\tau)d\tau \tag{2.4}$$

The right-hand side of (2.4) appears in another calculation, which extends the significance of the complex modulus. First, it must be agreed that of the many definitions of Fourier transform available, the following one must be used:

$$\begin{aligned} \mathcal{F}_t\{\varphi(t)\} &= \hat{\varphi}(\kappa) = \int_{-\infty}^{\infty} \exp(-i\kappa t)\varphi(t)dt \\ \varphi(t) &= \frac{1}{2\pi}\int_{-\infty}^{\infty} \exp(i\kappa t)\hat{\varphi}(\kappa)d\kappa \end{aligned} \tag{2.5}$$

where it is understood that a hat (^) over a symbol indicates the Fourier transform of the function denoted by that symbol, with respect to the independent variable (in this case, t) whose position in the argument list is taken by the transform parameter, κ. Thus

$\hat{\psi}(x, y, z, \kappa)$ is the Fourier transform with respect to t of the function $\psi(x, y, z, t)$. Using (2.5), the Fourier transform of the right-hand side of (2.1) is

$$\begin{aligned}
&\mathcal{F}_t\{\gamma(\underline{x}, t)*dE(t)\} \\
&= \int_{-\infty}^{\infty} \exp(i\kappa t)\Big\{\int_{-\infty}^{t} \gamma(\underline{x}, t-\tau)dE(\tau)\Big\}dt \\
&= \int_{0}^{\infty} \exp(i\kappa t)\Big\{E(0)\gamma(\underline{x}, t) + \int_{0}^{t}\gamma(\underline{x}, t-\tau)\dot{E}(\tau)d\tau\Big\}dt \\
&= E(0)\hat{\gamma}(\underline{x},\kappa) + \int_{0}^{\infty} \dot{E}(\tau) \int_{\tau}^{\infty}\exp(-i\kappa t)\gamma(\underline{x}, t-\tau)dtd\tau \\
&= E(0)\hat{\gamma}(\underline{x}, \kappa) + \int_{0}^{\infty} \dot{E}(\tau) \int_{0}^{\infty}\exp[-i\kappa(\tau+\tau')]\,\gamma(\underline{x}, \tau')d\tau'd\tau \\
&= \Big\{E(0) + \int_{0}^{\infty}\exp(-i\kappa\tau)\dot{E}(\tau)d\tau\Big\}\,\hat{\gamma}(\underline{x},\kappa)
\end{aligned}$$

Thus,

$$\mathcal{F}_t\{\gamma(\underline{x}, t)*dE(t)\} = \tilde{E}(\kappa)\hat{\gamma}(\underline{x}, \kappa) \qquad (2.6)$$

Equation (2.6) suggests that the concept of complex modulus need not be limited to real values of the frequency, ω; although the interpretation of complex modulus in connection with steady state response of a viscoelastic body is so limited. This observation predicts a usefulness of the complex modulus in cases other than steady state vibrations, although the nature of this usefulness won't become apparent until later (Chapters 4 and 5).

An elastic material is a special case of a viscoelastic material in the sense that its relaxation modulus has the form

$$E(t) = E\,H(t) \qquad (2.7)$$

where E is a constant, and H(t) is the unit step function

$$H(t) = 0 \quad -\infty < t < 0$$

$$H(t) = 1 \quad 0 \leq t < \infty$$

Using (2.7) in (2.1) gives the stress-strain relation for an elastic material as

$$\sigma(\underline{x}, t) = E\, \gamma(\underline{x}, t) \quad .$$

Furthermore, since $\dot{E}(t) = 0$ $(0 < t < \infty)$ for an elastic material, the complex modulus as defined by (2.4) is

$$\tilde{E}(\omega) = E(0) = E \quad .$$

It was mentioned that (2.1) governs a uniaxial stress state. Gurtin and Sternberg (ref. 10) have proved that the constitutive relations for any isotropic viscoelastic material in a multiaxial stress state can be written as follows:

$$\sigma_{ij}(\underline{x}, t) = 2\gamma_{ij}(\underline{x}, t) * d\mu(t) + \frac{1}{3}\,\delta_{ij}\gamma_{kk}(\underline{x}, t) * d[3K(t) - 2\mu(t)] \qquad (2.8)$$

where $\mu(t)$ is the relaxation modulus in shear, and $K(t)$ is the bulk relaxation modulus. $\sigma_{ij}(\underline{x}, t)$ and $\gamma_{ij}(\underline{x}, t)$ are components of the stress tensor, $\underline{\sigma}(\underline{x}, t)$, and the strain tensor, $\underline{\gamma}(\underline{x}, t)$, respectively. As in the case of an isotropic elastic solid, the behavior of an isotropic viscoelastic solid is completely determined by two material properties.

The relaxation modulus appearing in (2.1) governs a uniaxial stress state. It shall be called Young's relaxation modulus, E(t). It can be expressed in terms of $\mu(t)$ and K(t) through (2.8), in which $\underline{\sigma}(\underline{x}, t)$ is specified to be a uniaxial stress state. Solving (2.8) for the strain components, writing the relationship between the non-vanishing stress component and the corresponding strain component, and comparing with (2.1) gives

$$[E(t)]^{-1} = \frac{1}{9}\{3[\mu(t)]^{-1} + [K(t)]^{-1}\} \tag{2.9}$$

Equation (2.9) involves the Stieltjes inverse $[\varphi(t)]^{-1}$ of the function $\varphi(t)$, defined as follows:

$$[\varphi(t)]^{-1} * d\varphi(t) = H(t) \tag{2.10}$$

Equation (2.9) and the definition of complex modulus, (2.4) give a similar relation between the Young's complex modulus, the shear complex modulus, and the bulk complex modulus. Thus

$$\frac{1}{\tilde{E}(\omega)} = \frac{1}{9}\left\{\frac{3}{\tilde{\mu}(\omega)} + \frac{1}{\tilde{K}(\omega)}\right\}$$

or (2.11)

$$\tilde{E}(\omega) = \frac{9\tilde{K}(\omega)\tilde{\mu}(\omega)}{3\tilde{K}(\omega) + \tilde{\mu}(\omega)}$$

The Stieltjes convolution is an inconvenient operation to have to deal with in solving a boundary-initial value problem, since t cannot be eliminated from the problem merely by trying a solution of the form $f(\underline{x})\exp(i\omega t)$. Thus it is of great interest to be able to

express the relaxation modulus in such a way that the Stieltjes convolution can be eliminated from the problem. Such a representation is the exponential series.

$$E(t) = E_E + \sum_{k=1}^{N} E_k \exp(-t/\tau_k), \quad t \geq 0 \tag{2.12}$$

A relaxation modulus of the form of (2.12) results if one considers the material properties to be representable as a network of springs and dashpots. Bland (ref. 9) proposes as a basic hypothesis that "The microscopic structure of a linear viscoelastic material is mechanically equivalent to a network of linear viscous and elastic elements." (p. 19) The implication of such a hypothesis is that not only is (2.12) a good way to approximate the relaxation modulus of a viscoelastic material; it is the natural way. Whether or not one agrees with Bland's hypothesis, it is a fact that in principle one can represent any experimentally determined relaxation modulus, or complex modulus, to any desired degree of accuracy, by choosing N large enough in (2.12). In Appendix A, an experimentally determined complex modulus is represented as an exponential series in which N = 8.

The Stieltjes convolution of a function f(t) with the relaxation modulus E(t) as defined by (2.12) is

$$f(t)*dE(t) = \left[E_E + \sum_{k=1}^{N} E_k\right] f(t) - \sum_{k=1}^{N} \frac{E_k}{\tau_k} \exp\left(-\frac{t}{\tau_k}\right) \int_0^t \exp\left(\frac{\xi}{\tau_k}\right) f(\xi) d\xi$$

The derivative of order M of the Stieltjes convolution is

$$\frac{d^M}{dt^M}\left[f(t)*dE(t)\right] = \left[E_E + \sum_{k=1}^{N} E_k\right]\frac{d^M}{dt^M} f(t)$$

$$+ \sum_{m=1}^{M}\left[(-1)^m \sum_{k=1}^{N} \frac{E_k}{\tau_k^m}\,\frac{d^{M-m}}{dt^{M-m}} f(t)\right]$$

$$- (-1)^M \sum_{k=1}^{N} \frac{E_k}{\tau_k^{M+1}} \exp(-\frac{t}{\tau_k}) \int_0^t \exp(\frac{\xi}{\tau_k}) f(\xi)d\xi$$

The N terms,

$$\exp(-\frac{t}{\tau_k}) \int_0^t \exp(\frac{\xi}{\tau_k}) f(\xi)d\xi \qquad k = 1, 2, \ldots, N$$

are the only non-differential terms occurring in f(t)*dE(t), or in any of its derivatives. Hence there exists a differential operator, D, of order N, which when operating on any Stieltjes convolution involving E(t), results in differential terms exclusively. That operator is the following:

$$D[f(t)] = \left[\prod_{k=1}^{N} \tau_k\right]\frac{d^N}{dt^N} f(t) + \left[\sum_{j=1}^{N} \prod_{\substack{k=1 \\ k\neq j}}^{N} \tau_k\right]\frac{d^{N-1}}{dt^{N-1}} f(t)$$

$$+ \left[\sum_{j=1}^{N} \sum_{\substack{k=1 \\ k\neq j}}^{N} \prod_{\substack{\ell=1 \\ \ell\neq j,k}}^{N} \tau_\ell\right]\frac{d^{N-2}}{dt^{N-2}} f(t) + \ldots\ldots \qquad (2.13)$$

$$+ \left[\sum_{j=1}^{N} \sum_{\substack{k=1 \\ k\neq j}}^{N} \tau_j\tau_k\right]\frac{d^2}{dt^2} f(t) + \left[\sum_{k=1}^{N} \tau_k\right]\frac{d}{dt} f(t) + f(t)$$

When D operates on the Stieltjes convolution f(t)*dE(t), the result is:

$$D[f(t)*dE(t)] = E_E f(t) + \left[E_E \sum_{k=1}^{N} \tau_k + \sum_{k=1}^{N} \tau_k E_k\right] \frac{d}{dt} f(t)$$

$$+ \left[E_E \sum_{j=1}^{N} \sum_{\substack{k=1 \\ k\neq j}}^{N} \tau_j \tau_k + \sum_{j=1}^{N} \tau_j E_j \sum_{\substack{k=1 \\ k\neq j}}^{N} \tau_k\right] \frac{d^2}{dt^2} f(t) + \cdots\cdots$$

$$+ \left[E_E \sum_{j=1}^{N} \prod_{\substack{k=1 \\ k\neq j}}^{N} \tau_k + \sum_{j=1}^{N} \tau_j E_j \sum_{\substack{k=1 \\ k\neq j}}^{N} \prod_{\substack{\ell=1 \\ \ell\neq j,k}}^{N} \tau_\ell\right] \frac{d^{N-1}}{dt^{N-1}} f(t) \qquad (2.14)$$

$$+ \left[\prod_{j=1}^{N} \tau_j\right]\left[E_E + \sum_{k=1}^{N} E_k\right] \frac{d^N}{dt^N} f(t)$$

Consider now, D operating on exp(iωt) and on exp(iωt)*dE(t).

$$D[\exp(i\omega t)] = \left[\prod_{k=1}^{N} (1+i\omega\tau_k)\right] \exp(i\omega t)$$

$$D[\exp(i\omega t)*dE(t)] = \left\{E_E \prod_{k=1}^{N} (1+i\omega\tau_k) + \sum_{k=1}^{N} i\omega\tau_k E_k \prod_{\substack{\ell=1 \\ \ell\neq k}}^{N} (1+i\omega\tau_\ell)\right\} \exp(i\omega t) \qquad (2.15)$$

The complex modulus corresponding to the relaxation modulus (2.12) is (see (2.4)):

$$\tilde{E}(\omega) = E_E + \sum_{k=1}^{N} E_k - \sum_{k=1}^{N} \frac{E_k}{1+i\omega\tau_k}$$

or

$$\tilde{E}(\omega) = \frac{E_E \prod_{k=1}^{N} (1+i\omega\tau_k) + \sum_{k=1}^{N} i\omega\tau_k E_k \prod_{\substack{\ell=1 \\ \ell\neq k}}^{N} (1+i\omega\tau_\ell)}{\prod_{k=1}^{N} (1+i\omega\tau_k)} \qquad (2.16)$$

Comparing (2.15) and (2.16) one sees that $D[\exp(i\omega t)]/\exp(i\omega t)$ is the denominator of the complex modulus, and $D[\exp(i\omega t)*dE(t)]/\exp(i\omega t)$ is the numerator.

3. Derivation of Equations

The straightforward way to derive a set of equations governing a given boundary value problem, employing a given set of simplifying approximations, is to consider infinitesimal elements of the body, and sum the forces and moments acting on them. But in cases in which the number of forces and displacements under consideration is large, the geometry involved in this method gets complicated; and one worries, when he is finished, that he may have unintentionally left something out. Then the matter of choosing appropriate boundary conditions is at least as geometrically confusing as the deriving of the governing equations. This approach was used by Di Taranto (ref. 6) in deriving the equations for the three-layer beam.

Another way to derive the equations is to use an applicable variational principle. Although less straightforward than the above, in terms of fundamental laws of physics required, this method is much more systematic mathematically. Thus, once the simplifying approximations are incorporated into the variational principle, the deriving of the governing equations, as well as the natural boundary conditions, is a matter of routine mathematics.

For the purpose of deriving the equations governing the motion of a three-layer beam in which the middle layer is viscoelastic, an "applicable variational principle" is one which does not neglect inertia terms, and which allows the material properties to be viscoelastic. Gurtin, in ref. 11, presents variational principles involving dynamics of an elastic body; and in ref. 12, he presents

variational principles involving a viscoelastic body subject to quasi-static loading. The ideas presented in these two papers can be combined to give a variational principle involving both dynamics and viscoelastic material properties. This has been done in Appendix B.

The variational principle given in Appendix B defines the functional $\Phi\{S\}$ (B. 9) in which the state, S, must be kinematically admissible, as discussed in Appendix B. It was proved that if the variation of $\Phi\{S\}$ vanishes, the resulting state is the solution of the boundary-initial value problem under consideration. If, in addition to being kinematically admissible, further restrictions are placed on S, then setting the variation of $\Phi\{S\}$ equal to zero produces, rather than the exact solution, the best solution available considering the new restrictions. In order to use the variational principle to establish a useful approximate theory, S must be expressed in terms of unknown functions such that the desired approximations are taken into account. Then setting the variation of $\Phi\{S\}$ equal to zero results in a set of integral-differential relationships among the unknown functions as well as the natural boundary conditions and the initial conditions of the approximate theory.

The problem under consideration here concerns a beam subjected to transverse loading. The beam is constructed of three layers of homogeneous, isotropic material glued together so that there is no slippage between layers (Fig. 1). The outside layers are linearly elastic, whereas the middle layer is linearly viscoelastic. The width and depth of the beam are small in comparison with

its length; hence the following assumptions are justified (see refs. 13, 14):

(1) The predominant stress component in the outer layers is $\sigma_{11}(\underline{x}, t)$. All others can be neglected.

(2) Without making any assumptions concerning the relative bending stiffness of the middle layer with respect to the outer layers, the stress components $\sigma_{11}(\underline{x}, t)$ and $\sigma_{12}(\underline{x}, t)$ of the middle layer must both be included in the analysis. If, as will be assumed later, the bending stiffness of the middle layer is small compared to that of the other layers, the component $\sigma_{11}(\underline{x}, t)$ can be neglected (refs. 14, 15).

(3) The shear in the middle layer is uniformly distributed across the thickness of that layer (ref. 13).

These assumptions lead to the following representation of the displacement vector (see Fig. 2):

$$u_1(\underline{x}, t) = \begin{cases} \tilde{u}(x, t) - \frac{h_2}{2}\varphi(x, t) - (y - \frac{h_2}{2})v'(x, t) & ① \\ \tilde{u}(x, t) - y\varphi(x, t) & ② \\ \tilde{u}(x, t) + \frac{h_2}{2}\varphi(x, t) - (y + \frac{h_2}{2})v'(x, t) & ③ \end{cases} \qquad (3.1)$$

$$u_2(\underline{x}, t) = v(x, t) \qquad ①, ②, ③$$

$$u_3(\underline{x}, t) = 0 \qquad ①, ②, ③$$

Here, $\tilde{u}(x, t)$ is the displacement component in the axial direction, $v(x, t)$ is the displacement component in the transverse direction, and $\varphi(x, t)$ is the counter-clockwise rotation of point x on the reference

axis. The reference axis is defined as those points of the beam which, when the beam is at rest, lie on the x axis of the coordinate system shown in Fig. 2. The numbers ①, ②, and ③ refer to the layer of the beam in which the corresponding expression is valid.

Using the strain-displacement relations,

$$\gamma_{ij}(\underline{x}, t) = \frac{1}{2}[u_{i,j}(\underline{x}, t) + u_{j,i}(\underline{x}, t)]$$

and (3.1), the components of the strain tensor are obtained. The non-zero components are:

$$\gamma_{11}(\underline{x}, t) = \begin{cases} \tilde{u}'(x, t) - \frac{h_2}{2}\varphi'(x, t) - (y - \frac{h_2}{2})v''(x, t) & ① \\ \tilde{u}'(x, t) - y\varphi'(x, t) & ② \\ \tilde{u}'(x, t) + \frac{h_2}{2}\varphi'(x, t) - (y + \frac{h_2}{2})v''(x, t) & ③ \end{cases}$$

$$\gamma_{12}(\underline{x}, t) = \begin{cases} 0 & ① \\ \frac{1}{2}[v'(x, t) - \varphi(x, t)] & ② \\ 0 & ③ \end{cases} \qquad (3.2)$$

According to the assumptions (1) and (2), the normal stress components $\sigma_{22}(\underline{x}, t)$ and $\sigma_{33}(\underline{x}, t)$ are zero in all layers. Therefore, the relationship between the normal stress component $\sigma_{11}(\underline{x}, t)$ and the strain component $\gamma_{11}(\underline{x}, t)$ is the same as for a uniaxial stress state, i.e., (2.1). The relationship between $\sigma_{12}(\underline{x}, t)$ and $\gamma_{12}(\underline{x}, t)$ is obtained from (2.8). Hence,

$$\begin{aligned} \sigma_{11}(\underline{x}, t) &= \gamma_{11}(\underline{x}, t) * dE(t) \\ \sigma_{12}(\underline{x}, t) &= \gamma_{12}(\underline{x}, t) * d\mu(t) \end{aligned} \qquad (3.3)$$

where E(t) is Young's relaxation modulus, and $\mu(t)$ is the shear relaxation modulus for the appropriate layer. Equations (3.2) and (3.3) give the non-zero components of the stress tensor as

$$\sigma_{11}(\underline{x}, t) = \begin{cases} E_1\left[\tilde{u}'(x,t) - \frac{h_2}{2}\varphi'(x,t) - (y - \frac{h_2}{2})v''(x,t)\right] & ① \\ \left[\tilde{u}'(x,t) - y\varphi'(x,t)\right] * dE_2(t) & ② \\ E_3\left[\tilde{u}'(x,t) + \frac{h_2}{2}\varphi'(x,t) - (y + \frac{h_2}{2})v''(x,t)\right] & ③ \end{cases} \tag{3.4}$$

$$\sigma_{12}(\underline{x}, t) = \begin{cases} 0 & ① \\ \left[v'(x,t) - \varphi(x,t)\right] * d\mu_2(t) & ② \\ 0 & ③ \end{cases}$$

where the subscript attached to a relaxation modulus refers to the layer to which it applies, and a relaxation modulus with no time argument is a constant (elastic material).

In order to represent the vector field $\underline{f}(\underline{x}, t)$ defined by (B. 6), the following initial conditions must be specified:

$$\tilde{u}(x, 0) = \tilde{\underset{\sim}{u}}(x), \qquad \mathring{\tilde{u}}(x, 0) = \mathring{\tilde{\underset{\sim}{u}}}(x)$$

$$v(x, 0) = \underset{\sim}{v}(x), \qquad \mathring{v}(x, 0) = \mathring{\underset{\sim}{v}}(x) \tag{3.5}$$

$$\varphi(x, 0) = \underset{\sim}{\varphi}(x), \qquad \mathring{\varphi}(x, 0) = \mathring{\underset{\sim}{\varphi}}(x)$$

There are no body forces. The components of the vector $\underline{f}(\underline{x}, t)$ can now be written as follows:

$$f_1(\underline{x}, t) = \begin{cases} \rho_1 \{ t[\mathring{\tilde{\underset{\sim}{u}}}(x) - \frac{h_2}{2} \mathring{\underset{\sim}{\varphi}}(x) - (y - \frac{h_2}{2}) \mathring{\underset{\sim}{v}}'(x)] \\ \quad + [\tilde{\underset{\sim}{u}}(x) - \frac{h_2}{2} \underset{\sim}{\varphi}(x) - (y - \frac{h_2}{2}) \underset{\sim}{v}'(x)] \} & ① \\ \rho_2 \{ t[\mathring{\tilde{\underset{\sim}{u}}}(x) - y \mathring{\underset{\sim}{\varphi}}(x)] + [\tilde{\underset{\sim}{u}}(x) - y \underset{\sim}{\varphi}(x)] & ② \\ \rho_3 \{ t[\mathring{\tilde{\underset{\sim}{u}}}(x) + \frac{h_2}{2} \mathring{\underset{\sim}{\varphi}}(x) - (y + \frac{h_2}{2}) \mathring{\underset{\sim}{v}}'(x)] \\ \quad + [\tilde{\underset{\sim}{u}}(x) + \frac{h_2}{2} \underset{\sim}{\varphi}(x) - (y + \frac{h_2}{2}) \underset{\sim}{v}'(x)] \} & ③ \end{cases}$$

$$f_2(\underline{x}, t) = \begin{cases} \rho_1 \{ t \mathring{\underset{\sim}{v}}(x) + \underset{\sim}{v}(x) \} & ① \\ \rho_2 \{ t \mathring{\underset{\sim}{v}}(x) + \underset{\sim}{v}(x) \} & ② \\ \rho_3 \{ t \mathring{\underset{\sim}{v}}(x) + \underset{\sim}{v}(x) \} & ③ \end{cases}$$

$$f_3(\underline{x}, t) = 0 \qquad ①, ②, ③$$

where ρ_1, ρ_2, and ρ_3 are the densities of layers 1, 2, and 3, respectively.

The traction boundary conditions are illustrated in Fig. 3. The prescribed traction for the top surface of the beam is the distributed normal load p(x, t), which is uniformly distributed with respect to the width of the beam. Thus, for the top surface, the traction vector is

$$\overset{\circ}{s}_1(\underline{x}, t) = 0, \quad \overset{\circ}{s}_2(\underline{x}, t) = p(x, t), \quad \overset{\circ}{s}_3(\underline{x}, t) = 0$$
$$\text{for } x_1 = x, \; x_2 = h_1 + \frac{h_2}{2}, \; -\frac{b}{2} < x_3 < \frac{b}{2} \tag{3.7}$$

where b is the width of the beam. On all other lateral surfaces of the beam, the prescribed traction is zero; i.e., $\underline{\overset{\circ}{s}}(\underline{x}, t) = \underline{0}$. It has not been stated yet whether tractions or displacements will be prescribed on the ends of the beam. In order to be flexible later, it will be assumed for now that tractions are prescribed. If it is decided later that some component of displacement is to be prescribed at one end, then that portion of the boundary switches from B_2 to B_1, and the corresponding integral must be deleted from $\Phi\{S\}$. Let the prescribed tractions be $\underline{\overset{\circ}{s}}(\underline{x}, t)$, where $\underline{x}$ is the position vector of a point on one of the end surfaces of the beam, in this case. Referring to (3.1), (3.2), (3.4), (3.6), (3.7), and (B.9), $\Phi\{S\}$ can now be written as

$$\Phi\{S\} = \tfrac{1}{2}\int_R \{g(t)*d\sigma_{11}(\underline{x}, t)*d\gamma_{11}(\underline{x}, t)+2g(t)*d\sigma_{12}(\underline{x}, t)*d\gamma_{12}(\underline{x}, t)\}\,d\underline{x}$$

$$+\tfrac{1}{2}\int_R \rho(\underline{x})\{u_1(\underline{x}. t)*du_1(\underline{x}, t)+u_2(\underline{x}, t)*du_2(\underline{x}, t\}\,d\underline{x}$$

$$-\int_R \{f_1(\underline{x}, t)*du_1(\underline{x}, t)+f_2(\underline{x}, t)*du_2(\underline{x}, t)\}\,d\underline{x} \qquad (3.8)$$

$$-\int_0^L g(t)*dp(x, t)*dv(x, t)dx$$

$$-\int_{ENDS} \{g(t)*d\mathring{s}_1(\underline{x}, t)*du_1(\underline{x}, t)+g(t)*d\mathring{s}_2(\underline{x}, t)*du_2(\underline{x}, t)\}\,dx$$

In (3.8) R is used to denote the two dimensions of the beam shown in Fig. 2. Since none of the terms in (3.8) have anything to do with the width dimension, integration across the width results in the factor b (the width) occurring in every term. Since this factor can be divided out of $\Phi\{S\}$, it contributes nothing to the end result. Therefore it was simply left out of (3.8). Integration with respect to y is straightforward due to the form of representation of the terms in (3.8). When this is done it is evident that the actual distribution of surface tractions over the ends of the beam affects $\Phi\{S\}$ only in the form of certain integrals, clearly identifiable as components of resultant forces and moments acting on particular layers. These resultants are labelled according to the notation shown in Fig. 3.

Now, taking the variation of $\Phi\{S\}$ and setting it equal to zero produces the following results:

Governing equations:

$$
\begin{aligned}
&(h_1E_1+h_3E_3)\tilde{u}''(x,t)+h_2\tilde{u}''(x,t)*dE_2(t)\\
&\quad-\frac{h_2}{2}(h_1E_1-h_3E_3)\varphi''(x,t)-\tfrac{1}{2}(h_1^2E_1-h_3^2E_3)v'''(x,t)\\
&\quad-(\rho_1h_1+\rho_2h_2+\rho_3h_3)\ddot{\tilde{u}}(x,t)+\frac{h_2}{2}(\rho_1h_1-\rho_3h_3)\ddot{\varphi}(x,t)\\
&\quad+\tfrac{1}{2}(\rho_1h_1^2-\rho_3h_3^2)\ddot{v}'(x,t)=0\\
&\tfrac{1}{3}(h_1^3E_1+h_3^3E_3)v''''(x,t)-\tfrac{1}{3}(\rho_1h_1^3+\rho_3h_3^3)\ddot{v}''(x,t)\\
&\quad-h_2v''(x,t)*d\mu_2(t)+(\rho_1h_1+\rho_2h_2+\rho_3h_3)\ddot{v}(x,t)\\
&\quad-\tfrac{1}{2}(h_1^2E_1-h_3^2E_3)\tilde{u}'''(x,t)+\tfrac{1}{2}(\rho_1h_1^2-\rho_3h_3^2)\ddot{\tilde{u}}'(x,t) \qquad (3.9)\\
&\quad+\frac{h_2}{4}(h_1^2E_1+h_3^2E_3)\varphi'''(x,t)-\frac{h_2}{4}(\rho_1h_1^2+\rho_3h_3^2)\ddot{\varphi}'(x,t)\\
&\quad+h_2\varphi'(x,t)*d\mu_2(t)=p(x,t)\\
&\frac{h_2}{4}(h_1^2E_1+h_3^2E_3)v'''(x,t)-\frac{h_2}{4}(\rho_1h_1^2+\rho_3h_3^2)\ddot{v}'(x,t)\\
&\quad+h_2v'(x,t)*d\mu_2(t)-\frac{h_2}{2}(h_1E_1-h_3E_3)\tilde{u}''(x,t)\\
&\quad+\frac{h_2}{2}(\rho_1h_1-\rho_3h_3)\ddot{\tilde{u}}(x,t)+\frac{h_2^2}{4}(h_1E_1+h_3E_3)\varphi''(x,t)\\
&\quad+\frac{h_2^3}{12}\varphi''(x,t)*dE_2(t)-\frac{h_2^2}{12}(3\rho_1h_1+\rho_2h_2+3\rho_3h_3)\ddot{\varphi}(x,t)\\
&\quad-h_2\varphi(x,t)*d\mu_2(t)=0
\end{aligned}
$$

Natural boundary conditions:

(1) $\tilde{u}(x,t)$ or

$$N_1(x,t)+N_2(x,t)+N_3(x,t) = (h_1E_1+h_3E_3)\tilde{u}'(x,t)$$
$$+h_2\tilde{u}'(x,t)*dE_2(t) - \frac{h_2}{2}(h_1E_1-h_3E_3)\varphi'(x,t)$$
$$-\tfrac{1}{2}(h_1^2E_1-h_3^2E_3)v''(x,t)$$

(2) $v(x,t)$ or

$$Q(x,t) = -\tfrac{1}{3}(h_1^3E_1+h_3^3E_3)v'''(x,t) + \tfrac{1}{3}(\rho_1h_1^3+\rho_3h_3^3)\ddot{v}'(x,t)$$
$$+h_2v'(x,t)*d\mu_2(t) + \tfrac{1}{2}(h_1^2E_1-h_3^2E_3)\tilde{u}''(x,t) \qquad (3.10)$$
$$-\tfrac{1}{2}(\rho_1h_1^2-\rho_3h_3^2)\ddot{\tilde{u}}(x,t) - \frac{h_2}{4}(h_1^2E_1+h_3^2E_3)\varphi''(x,t)$$
$$+\frac{h_2}{4}(\rho_1h_1^2-\rho_3h_3^2)\ddot{\varphi}(x,t)-h_2\varphi(x,t)*d\mu_2(t)$$

(3) $v'(x,t)$ or

$$M_1(x,t)+M_3(x,t) + \frac{h_2}{2}[N_1(x,t)-N_3(x,t)] = \tfrac{1}{3}(h_1^3E_1+h_3^3E_3)v''(x,t)$$
$$-\tfrac{1}{2}(h_1^2E_1-h_3^2E_3)\tilde{u}'(x,t) + \frac{h_2}{4}(h_1^2E_1+h_3^2E_3)\varphi'(x,t)$$

(4) $\varphi(x,t)$ or

$$M_2(x,t) - \frac{h_2}{2}[N_1(x,t)-N_3(x,t)] = \frac{h_2^2}{4}(h_1E_1+h_3E_3)\varphi'(x,t)$$
$$+\frac{h_2^3}{12}\varphi'(x,t)*dE_2(t) - \frac{h_2}{2}(h_1E_1-h_3E_3)\tilde{u}'(x,t)$$
$$+\frac{h_2}{4}(h_1^2E_1+h_3^2E_3)v''(x,t)$$

One expression from each of the pairs of natural boundary conditions (3.10) must be specified at each end of the beam. The first member of each pair is one of the four displacement boundary conditions which may be specified; the second member is the alternative traction boundary condition.

It was mentioned above that if the bending stiffness of the middle layer is small compared with the bending stiffnesses of the outer layers, the stress component $\sigma_{11}(\underline{x}, t)$ in the middle layer can be neglected. Equations (3.9) and (3.10) can be adapted to this new assumption by setting $E_2(t) \equiv 0$. Unless the beam is vibrating at very high frequency, the major contribution to inertia will be from the term $\ddot{v}(x, t)$ (transverse inertia). All other inertia terms represent either rotatory inertia or axial inertia. These other inertia terms will be neglected. Finally, a great simplification of the governing equations, and boundary conditions, can be accomplished by imposing symmetry on the top and bottom layers of the beam, i.e.,

$$E_1 = E_3 = E_o, \quad h_1 = h_3 = h_o, \quad \rho_1 = \rho_3 = \rho_o$$

The subscript "o" stands for "outer". Similarly, properties which formerly had the subscript "2" will now have the subscript "M", which stands for "middle." This step uncouples $\tilde{u}(x, t)$ from $v(x, t)$ and $\varphi(x, t)$ in (3.9) and (3.10). For the loading and boundary conditions to be considered in this paper, $\tilde{u}(x, t)$ vanishes identically. Therefore, it may as well be deleted from the entire analysis, including (3.1), (3.2), and (3.4). Applying the above simplifications, (3.9)

and (3.10) reduce to:

Governing equations

$$\frac{2}{3}h_o^3E_o v''''(x,t) + \tfrac{1}{2}h_M h_o^2 E_o \varphi'''(x,t)$$

$$-h_M v''(x,t)*d\mu_M(t)+h_M\varphi'(x,t)*d\mu_M(t)$$

$$+(h_M\rho_M+2h_o\rho_o)\ddot{v}(x,t) = p(x,t) \qquad (3.11)$$

$$\tfrac{1}{2}h_M h_o^2 E_o v'''(x,t) + \tfrac{1}{2}h_M^2 h_o E_o \varphi''(x,t)$$

$$+h_M v'(x,t)*d\mu_M(t)-h_M\varphi(x,t)*d\mu_M(t) = 0$$

Natural boundary conditions:

(1) $v(x,t)$ or

$$Q(x,t) = -\frac{2}{3}h_o^3E_o v'''(x,t) - \tfrac{1}{2}h_M h_o^2 E_o \varphi''(x,t)$$

$$+h_M v'(x,t)*d\mu_M(t)-h_M\varphi(x,t)*d\mu_M(t)$$

(2) $v'(x,t)$ or

$$M_1(x,t)+M_3(x,t)+\tfrac{1}{2}h_M[N_1(x,t)-N_3(x,t)]$$

$$= \frac{2}{3}h_o^3E_o v''(x,t) + \tfrac{1}{2}h_M h_o^2 E_o \varphi'(x,t) \qquad (3.12)$$

(3) $\varphi(x,t)$ or

$$-\tfrac{1}{2}h_M[N_1(x,t)-N_3(x,t)]$$

$$= \tfrac{1}{2}h_M h_o^2 E_o v''(x,t) + \tfrac{1}{2}h_M^2 h_o E_o \varphi'(x,t)$$

4. Solution of Simply-Supported Three-Layer Beam

In this chapter, the problem of a simply-supported three-layer beam, in which the shear relaxation modulus of the middle layer is representable in the form of (2.12), is solved. Thus

$$\mu_M(t) = \mu_E + \sum_{k=1}^{N} \mu_k \exp(-\frac{t}{\tau_k}), \quad t \geq 0 \tag{4.1}$$

This problem has been chosen because it is solvable by a technique that has some resemblance to the eigenfunction expansion technique which would have been used had the beam been purely elastic. The solution of this problem reveals the nature of the effect viscoelasticity has on the beam; and sheds light on what to expect in solving the cantilever beam problem, which is considered in Chapter 5. The features of the simply-supported beam which make the proposed solution technique successful, also warn of the difficulty to be encountered if one were to apply this technique to the cantilever beam. The insight gained by studying this problem is of considerable value in constructing the solution of the cantilever beam.

In order to handle this problem most efficiently, it is useful to write the governing equations in terms of the linear operators L_1 and L_2, where

$$\begin{aligned} L_1[v(x,t), \varphi(x,t)] &= \frac{2}{3} h_o^3 E_o v''''(x,t) + \tfrac{1}{2} h_M h_o^2 E_o \varphi'''(x,t) \\ &\quad - h_M v''(x,t) * d\mu_M(t) + h_M \varphi'(x,t) * d\mu_M(t) \\ &\quad + (h_M \rho_M + 2h_o \rho_o) \ddot{v}(x,t) \end{aligned} \tag{4.2}$$

$$\begin{aligned} L_2[v(x,t), \varphi(x,t)] &= \tfrac{1}{2} h_M h_o^2 E_o v'''(x,t) + \tfrac{1}{2} h_M^2 h_o E_o \varphi''(x,t) \\ &\quad + h_M v'(x,t) * d\mu_M(t) - h_M \varphi(x,t) * d\mu_M(t) \end{aligned}$$

The governing equations, (3.11), can now be written as

$$\begin{aligned} L_1[v(x,t),\ \varphi(x,t)] &= p(x,t) \\ L_2[v(x,t),\ \varphi(x,t)] &= 0 \end{aligned} \tag{4.3}$$

Noting the choices available from (3.12), the boundary conditions applicable to the simply-supported beam are

$$\begin{aligned} B_1[v(x,t),\varphi(x,t)] &= v(0,t) \\ B_2[v(x,t),\varphi(x,t)] &= \tfrac{2}{3}h_o^3E_o v''(0,t) + \tfrac{1}{2}h_M h_o^2 E_o \varphi'(0,t) \\ B_3[v(x,t),\varphi(x,t)] &= \tfrac{1}{2}h_M h_o^2 E_o v''(0,t) + \tfrac{1}{2}h_M^2 h_o E_o \varphi'(0,t) \\ B_4[v(x,t),\varphi(x,t)] &= v(L,t) \\ B_5[v(x,t),\varphi(x,t)] &= \tfrac{2}{3}h_o^3E_o v''(L,t) + \tfrac{1}{2}h_M h_o^2 E_o \varphi'(L,t) \\ B_6[v(x,t),\varphi(x,t)] &= \tfrac{1}{2}h_M h_o^2 E_o v''(L,t) + \tfrac{1}{2}h_M^2 h_o E_o \varphi'(L,t) \end{aligned} \tag{4.4}$$

Let the boundary conditions be

$$B_j[v(x,t),\ \varphi(x,t)] = q_j(t) \quad (j = 1, 2, \ldots, 6) \tag{4.5}$$

where $q_j(t)$ $(j = 1, 2, \ldots, 6)$ are prescribed functions of time. Let the initial conditions be

$$v(x,0) = \underset{\sim}{v}(x), \quad \dot{v}(x,0) = \underset{\sim}{\dot{v}}(x) \tag{4.6}$$

where $\underset{\sim}{v}(x)$ and $\underset{\sim}{\dot{v}}(x)$ are prescribed functions of position. The complete boundary-initial value problem under consideration in this chapter is defined by (4.3), (4.5), and (4.6).

In general, the boundary conditions can be given any arbitrary,

time-dependent values. A method of handling beam problems with time-dependent boundary conditions was first presented by Mindlin and Goodman (ref. 16). This method was applied to the Timoshenko beam by Herrmann (ref. 17), and to the elastic three-layer beam by Yu (ref. 18). First, the problem is replaced by one with homogeneous boundary conditions, by means of the transformation

$$v(x,t) = w(x,t) + \sum_{j=1}^{6} g_{vj}(x)q_j(t)$$
$$\varphi(x,t) = \psi(x,t) + \sum_{j=1}^{6} g_{\varphi j}(x)q_j(t) \qquad (4.7)$$

The functions $g_{vj}(x)$ and $g_{\varphi j}(x)$ $(j = 1, 2, \ldots, 6)$ are chosen such that the boundary conditions (4. 4) applied to $w(x, t)$ and $\psi(x, t)$ vanish. There are infinitely many functions having this property. For convenience, these functions are usually taken to be polynomials. For the simply-supported beam, the following functions are satisfactory:

$$g_{v1}(x) = 1 - \frac{x}{L} \qquad g_{\varphi 1}(x) = 0$$

$$g_{v2}(x) = -\frac{L^2}{h_o^3 E_o}\left[2\frac{x}{L} - 3\frac{x^2}{L^2} + \frac{x^3}{L^3}\right] \qquad g_{\varphi 2}(x) = -\frac{3L}{h_M h_o^2 E_o}\left[2\frac{x}{L} - \frac{x^2}{L^2}\right]$$

$$g_{v3}(x) = \frac{L^2}{h_M h_o^2 E_o}\left[2\frac{x}{L} - 3\frac{x^2}{L^2} + \frac{x^3}{L^3}\right] \qquad g_{\varphi 3}(x) = \frac{4L}{h_M h_o E_o}\left[2\frac{x}{L} - \frac{x^2}{L^2}\right]$$

$$g_{v4}(x) = \frac{x}{L} \qquad g_{\varphi 4}(x) = 0$$

$$g_{v5}(x) = -\frac{L^2}{h_o^3 E_o}\left[\frac{x}{L} - \frac{x^3}{L^3}\right] \qquad g_{\varphi 5}(x) = -\frac{3L}{h_M h_o^2 E_o}\frac{x^2}{L^2}$$

$$g_{v6}(x) = \frac{L^2}{h_M h_o^2 E_o}\left[\frac{x}{L} - \frac{x^3}{L^3}\right] \qquad g_{\varphi 6}(x) = \frac{4L}{h_M h_o E_o}\frac{x^2}{L^2}$$

(4. 8)

Using (4.7) in (4.3), (4.5), and (4.6), the boundary-initial value problem governing $w(x,t)$ and $\psi(x,t)$ is

$$L_j[w(x,t),\ \psi(x,t)] = P_j(x,t) \qquad (j = 1,2)$$

where (4.9)

$$P_1(x,t) = p(x,t) - L_1\left[\sum_{j=1}^{6} g_{vj}(x)q_j(t),\ \sum_{j=1}^{6} g_{\varphi j}(x)q_j(t)\right]$$

$$P_2(x,t) = -L_2\left[\sum_{j=1}^{6} g_{vj}(x)q_j(t),\ \sum_{j=1}^{6} g_{\varphi j}(x)q_j(t)\right]$$

with boundary conditions

$$B_j[w(x,t),\ \psi(x,t)] = 0 \qquad (j = 1,2,\ldots,6) \tag{4.10}$$

and initial conditions

$$\begin{aligned} w(x,0) &= \underset{\sim}{w}(x) = \underset{\sim}{v}(x) - \sum_{j=1}^{6} g_{vj}(x)q_j(0) \\ \dot{w}(x,0) &= \dot{\underset{\sim}{w}}(x) = \dot{\underset{\sim}{v}}(x) - \sum_{j=1}^{6} g_{vj}(x)\dot{q}_j(0) \end{aligned} \tag{4.11}$$

While the functions $g_{vj}(x)$, $g_{\varphi j}(x)$ $(j = 1,2,\ldots,6)$ are not unique, this need not cause a non-uniqueness in $v(x,t)$ and $\varphi(x,t)$. The functions $w(x,t)$ and $\psi(x,t)$ are determined, dependent on the choice of $g_{vj}(x)$, $g_{\varphi j}(x)$ $(j = 1,2,\ldots,6)$ through (4.9) and (4.11), in such a way as to compensate for the non-uniqueness.

Once the problem has been transformed into one with homogeneous boundary conditions, the next step in the Mindlin-Goodman procedure would be to try to satisfy (4.9), (4.10), and (4.11) by

means of an eigenfunction expansion. To do this, one would propose that the homogeneous equations

$$L_j[w(x,t),\ \psi(x,t)] = 0 \qquad (j = 1, 2)$$

$$B_j[w(x,t),\ \psi(x,t)] = 0 \qquad (j = 1, 2, \ldots, 6)$$

have solutions of the form $W(x)\exp(i\omega t)$ and $\Psi(x)\exp(i\omega t)$. However, due to the presence of the Stieltjes convolution in the linear operators L_1 and L_2, functions of this form cannot satisfy the homogeneous equations. Thus, the first effect that viscoelasticity has on the problem is to cast doubt upon the applicability of the eigenfunction expansion technique. Once the problem has been solved, hindsight shows that, indeed, the eigenfunction expansion technique could have been applied to the simply-supported beam, although it could not have been applied to a beam having other boundary conditions. Since the problem of the simply-supported beam is being studied for the purpose of gaining insight into the solving of the cantilever beam problem, a technique which more closely resembles Green's function analysis, than eigenfunction expansion, will be used, although the latter will play a role in the construction of the Green's function.

The following reciprocal identity, relating two displacement histories of the beam, can be verified through integration by parts:

$$\int_0^L \{u(x,t)*L_1[w(x,t),\ \psi(x,t)] - \theta(x,t)*L_2[w(x,t),\psi(x,t)]\}dx$$

$$= \int_0^L \{w(x,t)*L_1[u(x,t),\theta(x,t)] - \psi(x,t)*L_2[u(x,t),\theta(x,t)]\}dx$$

$$+\{w(x,t)*[-\tfrac{2}{3}h_o^3E_o u'''(x,t) - \tfrac{1}{2}h_M h_o^2 E_o \theta''(x,t)$$

$$+h_M u'(x,t)*d\mu_M(t) - h_M\theta(x,t)*d\mu_M(t)]$$

$$-u(x,t)*[-\tfrac{2}{3}h_o^3E_o w'''(x,t) - \tfrac{1}{2}h_M h_o^2 E_o \psi''(x,t)$$

$$+h_M w'(x,t)*d\mu_M(t) - h_M\psi(x,t)*d\mu_M(t)]$$

$$+w'(x,t)*[\tfrac{2}{3}h_o^3E_o u''(x,t) + \tfrac{1}{2}h_M h_o^2 E_o \theta'(x,t)]$$

$$-u'(x,t)*[\tfrac{2}{3}h_o^3E_o w''(x,t) + \tfrac{1}{2}h_M h_o^2 E_o \psi'(x,t)]$$

$$+\psi(x,t)*[\tfrac{1}{2}h_M h_o^2 E_o u''(x,t) + \tfrac{1}{2}h_M^2 h_o E_o \theta'(x,t)]$$

$$-\theta(x,t)*[\tfrac{1}{2}h_M h_o^2 E_o w''(x,t) + \tfrac{1}{2}h_M^2 h_o E_o \psi'(x,t)]\}\Big|_0^L$$

$$+(h_M\rho_M + 2h_o\rho_o)\int_0^L [u(x,0)\dot{w}(x,t) + \dot{u}(x,0)w(x,t)$$

$$-w(x,0)\dot{u}(x,t) - \dot{w}(x,0)u(x,t)]\,dx \qquad (4.12)$$

This equation contains both Riemann convolutions and Stieltjes convolutions (ref. 10). Let f(t) and g(t) be two functions of t, defined for $0 \le t < \infty$. Then the Riemann convolution is

$$f(t)*g(t) = \int_0^t f(t-\tau)g(\tau)d\tau \ .$$

The Stieltjes convolution is

$$f(t)*dg(t) = \int_{-\infty}^t f(t-\tau)dg(\tau)$$

In the case of the Stieltjes convolution, $g(t)$ may be defined on the interval $-\infty < t < \infty$, although only functions defined on the interval $0 \leq t < \infty$ are encountered in this paper.

Let $u(x, t)$ and $\theta(x, t)$ satisfy

$$\begin{aligned} L_j[u(x,t),\ \theta(x,t)] &= 0 \qquad (j = 1, 2) \\ B_j[u(x,t),\ \theta(x,t)] &= 0 \qquad (j = 1, 2, \ldots, 6) \end{aligned} \tag{4.13}$$

$$u(x, 0) = 0, \qquad \dot{u}(x, 0) = \underset{\sim}{\dot{u}}(x) \tag{4.14}$$

Then, since $w(x, t)$ and $\psi(x, t)$ satisfy (4.9), (4.10), and (4.11), (4.12) becomes

$$\begin{aligned} \int_0^L \underset{\sim}{\dot{u}}(x) w(x, t)\,dx &= \int_0^L [\underset{\sim}{w}(x)\dot{u}(x, t) + \underset{\sim}{\dot{w}}(x) u(x, t)]\,dx \\ &+ \frac{1}{h_M \rho_M + 2h_o \rho_o} \int_0^L [u(x, t) * P_1(x, t) - \theta(x, t) * P_2(x, t)]\,dx \end{aligned} \tag{4.15}$$

Once $u(x, t)$ and $\theta(x, t)$ have been determined, the right-hand side of (4.15) is known. Eventually $\underset{\sim}{\dot{u}}(x)$ will be replaced by a δ-function, so that (4.15) will give $w(x, t)$ directly.

It was mentioned earlier that the presence of Stieltjes convolutions in the operators L_1 and L_2 prevents (4.13) from being treated as an eigenvalue problem. However, due to the form of $\mu_M(t)$, specified in (4.1), the Stieltjes convolutions can be removed from (4.13) by operating with the differential operator D (2.13). Doing this, a new problem, containing only differential terms, results:

$$D\{L_j[u(x,t),\ \theta(x,t)]\} = 0 \qquad (j = 1, 2)$$

$$D\{B_j[u(x,t),\ \theta(x,t)]\} = 0 \qquad (j = 1, 2, \ldots, 6) \tag{4.16}$$

This problem can be treated as an eigenvalue problem.

Note that if a pair of functions satisfies (4.13), it must also satisfy (4.16). Therefore, the set of all solutions of (4.16) must contain, as a subset, the set of all solutions of (4.13). Thus, a solution of (4.13) can be constructed as a summation of all the solutions of (4.16), each term multiplied by the appropriate coefficient. There is no guarantee that the evaluation of these coefficients will be straightforward; it turns out to be straightforward for the simply-supported beam, and not so for a beam of any other boundary condition.

Let

$$u(x,t) = U(x)\exp(i\omega t)$$

$$\theta(x,t) = \Theta(x)\exp(i\omega t) \tag{4.17}$$

Using this in (4.16), and dividing by

$$\left[\prod_{k=1}^{N}(1+i\omega\tau_k)\right]\exp(i\omega t)\ ,$$

the following set of ordinary differential equations and boundary conditions for $U(x)$ and $\Theta(x)$ results.

$$\frac{2}{3}h_o^3 E_o U''''(x) + \tfrac{1}{2}h_M h_o^2 E_o \Theta'''(x) - h_M \tilde{\mu}_M(\omega) U''(x)$$

$$+ h_M \tilde{\mu}_M(\omega) \Theta'(x) - (h_M \rho_M + 2h_o \rho_o)\omega^2 U(x) = 0$$

$$\frac{1}{2}h_M h_o^2 E_o U'''(x) + \frac{1}{2}h_M^2 h_o E_o \Theta''(x) + h_M \tilde{\mu}_M(\omega) U'(x) \qquad (4.18)$$

$$- h_M \tilde{\mu}_M(\omega)\, \Theta(x) = 0$$

$$U(0) = 0, \quad U''(0) = 0, \quad \Theta'(0) = 0$$

$$U(L) = 0, \quad U''(L) = 0, \quad \Theta'(L) = 0$$

This set of equations differs from the set of equations which would have resulted if the functions (4.17) had been used directly in (4.13) only in that the relaxation modulus is replaced by the complex modulus, $\tilde{\mu}_M(\omega)$.

$$\tilde{\mu}_M(\omega) = \frac{\mu_E \prod_{k=1}^{N} (1+i\omega\tau_k) + \sum_{k=1}^{N} i\omega\tau_k \mu_k \prod_{\substack{\ell=1 \\ \ell \neq k}}^{N} (1+i\omega\tau_\ell)}{\prod_{k=1}^{N} (1+i\omega\tau_k)} \qquad (4.19)$$

That this should happen follows from (2.15) and (2.16). In light of the fact that the complex modulus was introduced, in Chapter 2, as a material property which is useful in describing steady state response, the fact that it occurs in (4.18), associated with a non-steady boundary-initial value problem, constitutes an extension of its applicability. While in the steady state problem its argument, ω, took on only real values, no such limitation is imposed upon the complex modulus in (4.18). In fact, that the frequency, ω, should

take on complex values is the sort of phenomenon viscoelasticity is expected to contribute. Note from (4.17) that the imaginary part of a complex frequency results in an exponential decay factor.

From (2.6) it follows that if (4.13) were operated on by the Fourier transform (2.5), rather than by the differential operator D, the same set of equations and boundary conditions, (4.18), would result. This is a significant observation which will prove to be of value in the next chapter. It was pointed out earlier that in constructing a solution of (4.13) as a summation of solutions of (4.16), one faces the task of finding the appropriate coefficients. In the case of the simply-supported beam, this does not present much of a problem; but in the case of the cantilever beam, to be considered in the next chapter, it does. If in the cantilever case, one uses the Fourier transform in (4.16), rather than D, the coefficients are determined in the inversion process.

Let

$$h = \frac{h_M}{h_o}, \quad \rho = \frac{\rho_M}{\rho_o}, \quad c^2 = \frac{E_o}{\rho_o}, \quad G(\omega) = \frac{\tilde{\mu}_M(\omega)}{E_o} \tag{4.20}$$

The differential equations of (4.18) can be uncoupled, resulting in a sixth order ordinary differential equation.

$$\frac{d^6}{dx^6}U(x) - \frac{2G(\omega)}{hh_o^2}(4+6h+3h^2)\frac{d^4}{dx^4}U(x)$$

$$- \frac{6}{h_o^2}(2+h\rho)\frac{\omega^2}{c^2}\frac{d^2}{dx^2}U(x) + \frac{12G(\omega)}{hh_o^4}(2+h\rho)\frac{\omega^2}{c^2}U(x) = 0$$

$$\frac{d^6}{dx^6}\Theta(x) - \frac{2G(\omega)}{hh_o^2}(4+6h+3h^2)\frac{d^4}{dx^4}\Theta(x) \tag{4.21}$$

$$- \frac{6}{h_o^2}(2+h\rho)\frac{\omega^2}{c^2}\frac{d^2}{dx^2}\Theta(x) + \frac{12G(\omega)}{hh_o^4}(2+h\rho)\frac{\omega^2}{c^2}\Theta(x) = 0$$

These equations are satisfied by

$$U(x) = \sum_{j=1}^{3}[a_j \sin\lambda_j x + b_j \cos\lambda_j x]$$
$$\Theta(x) = \sum_{j=1}^{3}[a_j' \sin\lambda_j x + b_j' \cos\lambda_j x] \tag{4.22}$$

where a_j, b_j, a_j', b_j' $(j = 1, 2, 3)$ are arbitrary constants, and $\pm\lambda_j$ $(j = 1, 2, 3)$ are the six roots of the polynomial

$$\lambda^6 + \frac{2G(\omega)}{hh_o^2}(4+6h+3h^2)\lambda^4 - \frac{6}{h_o^2}(2+h\rho)\frac{\omega^2}{c^2}\lambda^2$$

$$- \frac{12G(\omega)}{hh_o^4}(2+h\rho)\frac{\omega^2}{c^2} = 0 \tag{4.23}$$

Although (4.22) satisfies (4.21), it does not necessarily satisfy (4.18). Substituting (4.22) into (4.18), it follows that the arbitrary constants of (4.22) must be related as follows:

$$a_j' = \frac{\lambda_j^2 - \frac{2G(\omega)}{h_o^2}}{h\lambda_j^2 + \frac{2G(\omega)}{h_o^2}}\lambda_j b_j, \quad b_j' = -\frac{\lambda_j^2 - \frac{2G(\omega)}{h_o^2}}{h\lambda_j^2 + \frac{2G(\omega)}{h_o^2}}\lambda_j a_j, \quad (j = 1, 2, 3)$$

Therefore, the differential equations of (4.18) are satisfied by

$$U(x) = \sum_{j=1}^{3} [a_j \sin\lambda_j x + b_j \cos\lambda_j x]$$

$$\Theta(x) = \sum_{j=1}^{3} \frac{\lambda_j^2 - \frac{2G(\omega)}{h_o^2}}{h\lambda_j^2 + \frac{2G(\omega)}{h_o^2}} \lambda_j [b_j \sin\lambda_j x - a_j \cos\lambda_j x] \qquad (4.24)$$

Applying the boundary conditions of (4.18) to (4.24), one gets

$$b_1 = b_2 = b_3 = 0$$

$$\begin{bmatrix} \sin\lambda_1 L & \sin\lambda_2 L & \sin\lambda_3 L \\ \lambda_1^2 \sin\lambda_1 L & \lambda_2^2 \sin\lambda_2 L & \lambda_3^2 \sin\lambda_3 L \\ \frac{1}{\lambda_1^2} \sin\lambda_1 L & \frac{1}{\lambda_2^2} \sin\lambda_2 L & \frac{1}{\lambda_3^2} \sin\lambda_3 L \end{bmatrix} \begin{Bmatrix} a_1 \\ a_2 \\ a_3 \end{Bmatrix} = \begin{Bmatrix} 0 \\ 0 \\ 0 \end{Bmatrix} \qquad (4.25)$$

The determinant must vanish in order for a non-trivial solution to exist. Therefore,

$$\left(\frac{\lambda_1^2}{\lambda_2^2} - \frac{\lambda_2^2}{\lambda_1^2} + \frac{\lambda_2^2}{\lambda_3^2} - \frac{\lambda_3^2}{\lambda_2^2} + \frac{\lambda_3^2}{\lambda_1^2} - \frac{\lambda_1^2}{\lambda_3^2}\right) \sin\lambda_1 L \sin\lambda_2 L \sin\lambda_3 L = 0 \qquad (4.26)$$

The eigenvalue parameter of (4.18) is ω. The parameters λ_1, λ_2, and λ_3 are dependent upon ω through (4.23). Since the characteristic equation, (4.26), is written in terms of λ_1, λ_2, and λ_3, the finding of the eigenvalues requires solving (4.23) and (4.26) simultaneously. By inspection, (4.26) is satisfied if one of the three parameters λ_1, λ_2, or λ_3, say λ_k, has a value such that

$$\sin\lambda_k L = 0 \quad .$$

Since λ_1, λ_2, and λ_3 are defined as the three independent roots of (4.23), there is no designation as to which root goes with which symbol, λ_1, λ_2, or λ_3. Thus, the roots can be renamed so that the above equation applies to λ_1. This equation is satisfied when

$$\lambda_1 = \frac{n\pi}{L} \quad , \qquad n = 1, 2, \ldots .$$

A frequency, ω, for which $\lambda_1 = \frac{n\pi}{L}$ can be found by setting $\lambda = \frac{n\pi}{L}$ in (4.23), and using (4.19).

$$\left[\frac{n^6\pi^6}{L^6} - \frac{6(2+h\rho)}{h_o^2 c^2}\,\frac{n^2\pi^2}{L^2}\,\omega^2\right]\prod_{k=1}^{N}(1+i\omega\tau_k)$$
$$+\frac{1}{E_o}\left[\frac{2(4+6h+3h^2)}{h h_o^2}\,\frac{n^4\pi^4}{L^4} - \frac{12(2+h\rho)}{h h_o^4 c^2}\,\omega^2\right]$$
$$\cdot\left[\mu_E\prod_{k=1}^{N}(1+i\omega\tau_k) + \sum_{k=1}^{N} i\omega\tau_k\mu_k \prod_{\substack{\ell=1\\ \ell\neq k}}^{N}(1+i\omega\tau_\ell)\right] = 0 \qquad (4.27)$$

$$(n = 1, 2, \ldots\ldots)$$

For each fixed value of n, this is a polynomial of order N+2 for the frequency, ω, and therefore, N+2 eigenvalues exist for each value of n. All the eigenvalues of (4.18) can be found from (4.27). Let them be named ω_{nm}, $(m = 1, 2, \ldots, N+2)$, $(n = 1, 2, \ldots .)$.

For any given eigenvalue, ω_{nm}, the corresponding parameters λ_{jnm} $(j = 1, 2, 3)$ are found using (4.23). Let the root $\frac{n\pi}{L}$ be called λ_{1nm}. Using these values of λ_{jnm} $(j = 1, 2, 3)$ in (4.25) gives $a_2 = a_3 = 0$. Note, therefore, that λ_{2nm} and λ_{3nm} do not appear in the eigen-

functions. Let $a_1 = 1$. Then, using (4.24), the eigenfunctions corresponding to the eigenvalue ω_{nm} are

$$U_{nm}(x) = \sin \frac{n\pi x}{L}$$

$$\Theta_{nm}(x) = -\frac{n\pi}{L} \frac{\frac{n^2\pi^2}{L^2} - \frac{2G(\omega_{nm})}{h_o^2}}{h\frac{n^2\pi^2}{L^2} + \frac{2G(\omega_{nm})}{h_o^2}} \cos \frac{n\pi x}{L} \tag{4.28}$$

Using (4.17) and (4.28), the solutions of (4.16) are

$$u_{nm}(x,t) = \sin \frac{n\pi x}{L} \exp(i\omega_{nm} t)$$

$$\theta_{nm}(x,t) = -\frac{n\pi}{L} \frac{\frac{n^2\pi^2}{L^2} - \frac{2G(\omega_{nm})}{h_o^2}}{h\frac{n^2\pi^2}{L^2} + \frac{2G(\omega_{nm})}{h_o^2}} \cos \frac{n\pi x}{L} \exp(i\omega_{nm} t) \tag{4.29}$$

$$(m = 1, 2, \ldots, N+2), \quad (n = 1, 2, \ldots .)$$

Then, the solution of (4.13) can be expressed as a combination of the functions of (4.29),

$$u(x,t) = \sum_{n=1}^{\infty} d_n \sum_{m=1}^{N+2} c_{nm} u_{nm}(x,t)$$

$$\theta(x,t) = \sum_{n=1}^{\infty} d_n \sum_{m=1}^{N+2} c_{nm} \theta_{nm}(x,t) \tag{4.30}$$

where the coefficients d_n, c_{nm} are not yet determined. Applying the linear operators L_1 and L_2 to (4.30), and using (4.1) and (4.23), one gets

$$L_1[u(x,t),\theta(x,t)] =$$

$$h_M(1+h)\sum_{n=1}^{\infty}\sum_{m=1}^{N+2}\sum_{k=1}^{N}\frac{n^4\pi^4}{L^4}\sin\frac{n\pi x}{L}\,\frac{d_n c_{nm}\mu_k \exp(-t/\tau_k)}{(1+i\omega_{nm}\tau_k)\left[h\frac{n^2\pi^2}{L^2}+\frac{2G(\omega_{nm})}{h_o^2}\right]} \tag{4.31}$$

$$L_2[u(x,t),\theta(x,t)] =$$

$$h_M(1+h)\sum_{n=1}^{\infty}\sum_{m=1}^{N+2}\sum_{k=1}^{N}\frac{n^3\pi^3}{L^3}\cos\frac{n\pi x}{L}\,\frac{d_n c_{nm}\mu_k \exp(-t/\tau_k)}{(1+i\omega\tau_k)\left[h\frac{n^2\pi^2}{L^2}+\frac{2G(\omega_{nm})}{h_o^2}\right]}$$

The right-hand side of (4.31) must vanish for $t \geq 0$, and for $0 \leq x \leq L$. The coefficients, d_n, c_{nm} must be picked such that this happens. Because the x dependence in (4.31) is independent of the index m, this can be done by choosing the constants, c_{nm}, such that

$$\sum_{m=1}^{N+2}\frac{c_{nm}}{(1+i\omega_{nm}\tau_k)\left[h\frac{n^2\pi^2}{L^2}+2\frac{G(\omega_{nm})}{h_o^2}\right]} = 0 \tag{4.32}$$

$$(k = 1, 2, \ldots, N),\ (n = 1, 2, \ldots)$$

For a given value of n, these are N equations which must be satisfied by the N+2 constants, c_{nm}. Thus there is still the flexibility to impose two more conditions on the constants. Looking ahead to the initial conditions which must eventually be satisfied, a convenient choice for those two remaining conditions is

$$\sum_{m=1}^{N+2} c_{nm} = 0, \quad \sum_{m=1}^{N+2} i\omega_{nm} c_{nm} = 1 \qquad (n = 1, 2, \ldots) \tag{4.33}$$

Using (4.32) and (4.33) to define the constants, c_{nm}, (4.30) satisfies (4.13) for any choice of the constants d_n. Note that the finding of the constants c_{nm} reduces to solving (4.32) and (4.33) due to the fact that the eigenfunctions (4.28) corresponding to an eigenvalue ω_{nm}, have an x dependence which is independent of the index m. This does not happen for any boundary conditions other than simply supported.

The initial values of u(x, t), using (4.29), (4.30), and (4.33) are

$$u(x, 0) = 0, \quad \dot{u}(x, 0) = \sum_{n=1}^{\infty} d_n \sin \frac{n\pi x}{L}$$

These can be matched to the initial conditions of (4.14) by expanding $\underset{\sim}{\dot{u}}(x)$ in a Fourier sine series. This gives

$$d_n = \frac{2}{L} \int_0^L \underset{\sim}{\dot{u}}(x) \sin \frac{n\pi x}{L} \, dx$$

Using (4.29) and (4.30)

$$u(x,t) = \sum_{n=1}^{\infty} \frac{2}{L} \sin\frac{n\pi x}{L} \int_0^L \underset{\sim}{u}(\xi) \sin\frac{n\pi\xi}{L}\, d\xi \sum_{m=1}^{N+2} c_{nm} \exp(i\omega_{nm} t)$$

$$\theta(x,t) = -\sum_{n=1}^{\infty} \frac{2}{L}\frac{n\pi}{L} \cos\frac{n\pi x}{L} \int_0^L \underset{\sim}{u}(\xi) \sin\frac{n\pi\xi}{L}\, d\xi$$

$$\cdot \sum_{m=1}^{N+2} c_{nm} \frac{\frac{n^2\pi^2}{L^2} - \frac{2G(\omega_{nm})}{h_o^2}}{h\frac{n^2\pi^2}{L^2} + \frac{2G(\omega_{nm})}{h_o^2}} \exp(i\omega_{nm} t) \qquad (4.34)$$

Note from (4.1) that for an elastic material, N = 0. Therefore, if the middle layer were elastic (4.27) would produce, for each n, two real frequencies, one the negative of the other. For a viscoelastic middle layer ($N \geq 1$), consider the substitution $\nu = i\omega$ in (4.27). Then, for each n, (4.27) becomes a polynomial of order N+2, in ν, in which all the coefficients are real and positive. The roots, therefore, are either real or complex, occurring in complex conjugate pairs. Since $\omega = -i\nu$, the roots of (4.27) are either pure imaginary or complex, occurring in pairs in which one is the negative complex conjugate of the other. These roots occur in (4.34) as $\exp(i\omega t)$. Thus, pure imaginary frequencies represent pure exponential decay, while complex frequencies, $\omega = \omega_1 + i\omega_2$, represent sinusoidal motion of frequency ω_1, with an exponentially decaying amplitude. Let the symbol $\bar{a}$ represent the complex conjugate of a. Using (4.19), (4.20),

$$G(-\bar{\omega}) = \overline{G(\omega)}$$

Using this, (4.32), and (4.33), it can be shown, using determinants, that if ω_{nm} is a pure imaginary frequency, then c_{nm} is real. Also, if ω_{np} and ω_{nq} are a pair of negative complex conjugate frequencies ($\omega_{nq} = -\overline{\omega_{np}}$), then c_{np} and c_{nq} are complex conjugates ($c_{np} = \overline{c_{nq}}$). Therefore, although the right-hand side of (4.34) involves complex functions, they add up in such a way that $u(x,t)$ and $\theta(x,t)$ are real.

Now that $u(x,t)$ and $\theta(x,t)$ are known, through (4.34), (4.32), (4.33), and (4.27), they can be used to determine $w(x,t)$, by use of (4.15). The easiest way to do this is to let $\underset{\sim}{u}(x) = \delta(x-\xi)$. Use this in (4.34) to get $u(x,\xi,t)$ and $\theta(x,\xi,t)$; then interchange ξ and x.

$$u(\xi,x,t) = \frac{2}{L}\sum_{n=1}^{\infty} \sin\frac{n\pi x}{L} \sin\frac{n\pi\xi}{L} \sum_{m=1}^{N+2} c_{nm}\exp(i\omega_{nm}t)$$

$$\theta(\xi,x,t) = -\frac{2}{L}\sum_{n=1}^{\infty} \frac{n\pi}{L} \sin\frac{n\pi x}{L} \cos\frac{n\pi\xi}{L} \tag{4.35}$$

$$\cdot \sum_{m=1}^{N+2} c_{nm} \frac{\frac{n^2\pi^2}{L^2} - \frac{2G(\omega_{nm})}{h_o^2}}{h\frac{n^2\pi^2}{L^2} + \frac{2G(\omega_{nm})}{h_o^2}} \exp(i\omega_{nm}t)$$

Since x and ξ were interchanged, integration in (4.15) is with respect to ξ rather than x. Therefore,

$$w(x,t) = \int_0^L [\underset{\sim}{w}(\xi)\underset{\sim}{u}(\xi,x,t) + \underset{\sim}{\dot{w}}(\xi)u(\xi,x,t)]\,d\xi$$

$$+ \frac{1}{h\rho_M M + 2h_o\rho_o} \int_0^L [u(\xi,x,t)*P_1(\xi,t) - \theta(\xi,x,t)*P_2(\xi,t)]\,d\xi \tag{4.36}$$

or

$$w(x,t) = \sum_{n=1}^{\infty} \sin\frac{n\pi x}{L} \sum_{m=1}^{N+2} A_{nm}(t) \tag{4.37}$$

where

$$A_{nm}(t) = \frac{2}{L} c_{nm}\Bigg\{\exp(i\omega_{nm}t)\int_0^L [\dot{\underset{\sim}{w}}(\xi)+i\omega_{nm}\underset{\sim}{w}(\xi)]\sin\frac{n\pi\xi}{L}\,d\xi$$

$$+ \frac{1}{h_M\rho_M+2h_o\rho_o}\exp(i\omega_{nm}t)^*\int_0^L\Bigg[P_1(\xi,t)\sin\frac{n\pi\xi}{L} \tag{4.38}$$

$$+ \frac{n\pi}{L}\,\frac{\frac{n^2\pi^2}{L^2}-\frac{2G(\omega_{nm})}{h_o^2}}{h\frac{n^2\pi^2}{L^2}+\frac{2G(\omega_{nm})}{h_o^2}}\,P_2(\xi,t)\cos\frac{n\pi\xi}{L}\Bigg]d\xi\Bigg\}$$

At this point, $v(x,t)$ can be obtained from (4.7), (4.37), and (4.38). Usually this is all one wants, since it is the transverse displacement that is most easily measured experimentally. However, in order to claim that the boundary-initial value problem of (4.3), (4.5), and (4.6) has been solved, $\varphi(x,t)$ must also be known. An expression for $\psi(x,t)$ in terms of $w(x,t)$, $P_1(x,t)$, $P_2(x,t)$, all of which are known, can be obtained from (4.9).

$$\psi(x,t)^*d\mu_M(t)^*d\mu_M(t) = -\frac{hh_o^4E_o^2}{12(1+h)}\frac{d^5}{dx^5}w(x,t)$$

$$+\frac{1}{2}h_o^2E_o(1+h)\frac{d^3}{dx^3}w(x,t)^*d\mu_M(t)$$

$$+\frac{d}{dx}w(x,t)^*d\mu_M(t)^*d\mu_M(t) - \frac{hh_o^2\rho_oE_o(2+h\rho)}{2(1+h)}\frac{d}{dx}\dot{w}(x,t)$$

$$-\frac{1}{hh_o}P_2(x,t)^*d\mu_M(t)+\frac{hh_oE_o}{2(1+h)}\frac{d}{dx}P_1(x,t)-\frac{h_oE_o}{2(1+h)}\frac{d^2}{dx^2}P_2(x,t)$$

Using (4. 37), (4. 38), (4. 23), (4. 32), (4. 33), and the equations for expanding a function as a Fourier sine series, or a Fourier cosine series, this can be reduced to

$$\psi(x,t) = -\sum_{n=1}^{\infty} \frac{n\pi}{L} \cos\frac{n\pi x}{L} \sum_{m=1}^{N+2} \frac{\frac{n^2\pi^2}{L^2} - \frac{2G(\omega_{nm})}{h_o^2}}{h\frac{n^2\pi^2}{L^2} + \frac{2G(\omega_{nm})}{h_o^2}} A_{nm}(t)$$

$$- \frac{4}{hh_o^3 E_o L} \sum_{n=1}^{\infty} \cos\frac{n\pi x}{L} \frac{\int_0^L P_2(\xi,t)\cos\frac{n\pi\xi}{L}d\xi}{h\frac{n^2\pi^2}{L^2} + \frac{2}{h_o^2 E_o}\left[\mu_E + \sum_{k=1}^{N}\mu_k\right]} \qquad (4.39)$$

From (4. 7), (4. 37), and (4.,39) v(x, t) and $\varphi(x, t)$ can be obtained.

$$v(x,t) = \sum_{j=1}^{6} g_{vj}(x)q_j(t) + \sum_{n=1}^{\infty} \sin\frac{n\pi x}{L} \sum_{m=1}^{N+2} A_{nm}(t)$$

$$\varphi(x,t) = \sum_{j=1}^{6} g_{\varphi j}(x)q_j(t) - \sum_{n=1}^{\infty} \frac{n\pi}{L}\cos\frac{n\pi x}{L} \sum_{m=1}^{N+2} \frac{\frac{n^2\pi^2}{L^2} - \frac{2G(\omega_{nm})}{h_o^2}}{h\frac{n^2\pi^2}{L^2} + \frac{2G(\omega_{nm})}{h_o^2}} A_{nm}(t)$$

$$- \frac{4}{hh_o^3 E_o L} \sum_{n=1}^{\infty} \cos\frac{n\pi x}{L} \frac{\int_0^L P_2(\xi,t)\cos\frac{n\pi\xi}{L}d\xi}{h\frac{n^2\pi^2}{L^2} + \frac{2}{h_o^2 E_o}\left[\mu_E + \sum_{k=1}^{N}\mu_k\right]} \qquad (4.40)$$

5. Solution of Cantilever Three-Layer Beam

In the preceding chapter, the problem of a simply-supported three-layer beam was solved. A major feature of the solution technique was the removing of the Stieltjes convolution by operating on (4.13) with the differential operator D, and then forming the solution of (4.13) as a combination of all the solutions of the transformed problem. While it was pointed out that if this technique were to be applied to the cantilever, great difficulty would be encountered in trying to find the correct combination of solutions of the transformed problem, it was also pointed out that if the Fourier transform had been applied to (4.13), rather than D, the same set of equations would have resulted. From this it can be inferred that these two methods of removing the Stieltjes convolution, D and the Fourier transform, are equivalent. But, while the former method includes no systematic method of choosing the correct combination of solutions of the transformed problem to satisfy the original boundary-initial value problem, the Fourier transform does. Therefore, the Fourier transform (2.5) will be used in this chapter.

The boundary-initial value problem to be considered in this chapter is again governed by (4.3), (4.5), and (4.6), except that the boundary operators, $B_j[v(x,t), \varphi(x,t)]$ $(j = 1, 2, \ldots, 6)$, must be chosen such that they describe a cantilever beam. Noting the choices available in (3.12), a cantilever with its fixed end at $x = 0$ and its free end at $x = L$ is described by the following choice of boundary operators.

$$B_1[v(x,t),\ \varphi(x,t)] = v(0,t)$$

$$B_2[v(x,t),\varphi(x,t)] = v'(0,t)$$

$$B_3[v(x,t),\ \varphi(x,t)] = \varphi(0,t)$$

$$\begin{aligned} B_4[v(x,t),\ \varphi(x,t)] &= -\frac{2}{3}h_o^3E_o v'''(L,t) - \frac{1}{2}h_M h_o^2 E_o \varphi''(L,t) \\ &\quad + h_M v'(L,t)*d\mu_M(t) - h_M\varphi(L,t)*d\mu_M(t) \end{aligned} \tag{5.1}$$

$$B_5[v(x,t),\ \varphi(x,t)] = \frac{2}{3}h_o^3E_o v''(L,t) + \frac{1}{2}h_M h_o^2 E_o \varphi'(L,t)$$

$$B_6[v(x,t),\ \varphi(x,t)] = \frac{1}{2}h_M h_o^2 E_o v''(L,t) + \frac{1}{2}h_M^2 h_o E_o \varphi'(L,t)$$

Again the transformation (4.7) is used, with $g_{vj}(x), g_{\varphi j}(x) (j=1, 2, \ldots, 6)$ chosen such that the boundary conditions for $w(x,t)$ and $\psi(x,t)$ are homogeneous. A suitable set of functions follows:

$$g_{v1}(x) = 1 \qquad g_{\varphi 1}(x) = 0$$

$$g_{v2}(x) = \frac{L}{4}\left[4\frac{x}{L} - 6\frac{x^2}{L^2} + 4\frac{x^3}{L^3} - \frac{x^4}{L^4}\right] \qquad g_{\varphi 2}(x) = 0$$

$$g_{v3}(x) = 0 \qquad g_{\varphi 3}(x) = 1 - 3\frac{x}{L} + 3\frac{x^2}{L^2} - \frac{x^3}{L^3}$$

$$g_{v4}(x) = -\frac{L^3}{16h_o^3E_o}\left[6\frac{x^2}{L^2} - 8\frac{x^3}{L^3} + 3\frac{x^4}{L^4}\right] \qquad g_{\varphi 4}(x) = 0 \tag{5.2}$$

$$g_{v5}(x) = -\frac{3L^2}{2h_o^3E_o}\left[4\frac{x^2}{L^2} - 4\frac{x^3}{L^3} + \frac{x^4}{L^4}\right] \qquad g_{\varphi 5}(x) = \frac{6L}{h_M h_o^2 E_o}\left[2\frac{x}{L} - 3\frac{x^2}{L^2} + \frac{x^3}{L^3}\right]$$

$$g_{v6}(x) = \frac{3L^2}{2h_M h_o^2 E_o}\left[4\frac{x^2}{L^2} - 4\frac{x^3}{L^3} + \frac{x^4}{L^4}\right] \qquad g_{\varphi 6}(x) = -\frac{8L}{h_M^2 h_o E_o}\left[2\frac{x}{L} - 3\frac{x^2}{L^2} + \frac{x^3}{L^3}\right]$$

Then $w(x, t)$ and $\psi(x, t)$ are again governed by the boundary-initial value problem of (4.9), (4.10), and (4.11). Let $u(x, t)$ and $\theta(x, t)$ be governed by the following boundary-initial value problem, in which A_1 and A_2 are arbitrary constants.

$$\begin{aligned} &L_j[u(x,t), \theta(x,t)] = A_j \delta(x-x_o)\delta(t) \qquad (j = 1, 2) \\ &B_j[u(x,t), \theta(x,t)] = 0 \qquad (j = 1, 2, \ldots, 6) \\ &u(x, 0) = 0, \quad \dot{u}(x, 0) = 0 \end{aligned} \tag{5.3}$$

Then the reciprocal identity (4.12) reduces to

$$\begin{aligned} A_1 w(x_o, t) - A_2 \psi(x_o, t) = &\int_0^L [u(x,t)*P_1(x,t) - \theta(x,t)*P_2(x,t)]\, dx \\ &+(h_M\rho_M+2h_o\rho_o) \int_0^L [\underset{\sim}{w}(x)\dot{u}(x,t)+\dot{\underset{\sim}{w}}(x)u(x,t)]\, dx. \end{aligned} \tag{5.4}$$

The reason (5.3) was chosen as the governing boundary-initial value problem, rather than (4.13) and (4.14), is that both $w(x_o, t)$ and $\psi(x_o, t)$ can be found directly (by choosing A_1, A_2 to be 1, 0 and 0, -1, respectively) rather than only $w(x_o, t)$, as was the case in Chapter 4.

Taking the Fourier transform, (2.5), with respect to t, of (5.3), the following set of ordinary differential equations and boundary conditions results.

$$\frac{2}{3} h_o^3 E_o \hat{u}''''(x,\kappa) + \frac{1}{2} h_M h_o^2 E_o \hat{\theta}'''(x,\kappa) - h_M \tilde{\mu}_M(\kappa) \hat{u}''(x,\kappa)$$

$$+ h_M \tilde{\mu}_M(\kappa) \hat{\theta}'(x,\kappa) - (h_M \rho_M + 2h_o \rho_o) \kappa^2 \hat{u}(x,\kappa) = A_1 \delta(x-x_o)$$

$$\frac{1}{2} h_M h_o^2 E_o \hat{u}'''(x,\kappa) + \frac{1}{2} h_M^2 h_o E_o \hat{\theta}''(x,\kappa) + h_M \tilde{\mu}_M(\kappa) \hat{u}'(x,\kappa)$$

$$- h_M \tilde{\mu}_M(\kappa) \hat{\theta}(x,\kappa) = A_2 \delta(x-x_o) \qquad (5.5)$$

$$\hat{u}(0,\kappa) = 0, \quad \hat{u}'(0,\kappa) = 0, \quad \hat{\theta}(0,\kappa) = 0$$

$$- \frac{2}{3} h_o^3 E_o \hat{u}'''(L,\kappa) - \frac{1}{2} h_M h_o^2 E_o \hat{\theta}''(L,\kappa) + h_M \tilde{\mu}_M(\kappa) \hat{u}'(L,\kappa)$$

$$- h_M \tilde{\mu}_M(\kappa) \hat{\theta}(L,\kappa) = 0$$

$$\hat{u}''(L,\kappa) = 0, \quad \hat{\theta}'(L,\kappa) = 0$$

If the differential equations of (5.5) were homogeneous, they would be the same as (4.21), incorporating the notation of (4.20). Therefore, the complementary functions corresponding to (5.5) must be the same as (4.24).

$$\hat{u}_c(x,\kappa) = \sum_{j=1}^{3} [a_j \sin\lambda_j x + b_j \cos\lambda_j x]$$

$$\hat{\theta}_c(x,\kappa) = \sum_{j=1}^{3} \frac{\lambda_j^2 - \frac{2G(\kappa)}{h_o^2}}{h\lambda_j^2 + \frac{2G(\kappa)}{h_o^2}} \lambda_j [b_j \sin\lambda_j x - a_j \cos\lambda_j x] \qquad (5.6)$$

The coefficients $a_j, b_j (j=1, 2, 3)$ are functions of the transform parameter κ, and $\pm\lambda_j (j = 1, 2, 3)$ are the six roots of (4.23). The particular solutions of (5.5) can be found by variation of parameters.

$$\hat{u}_p(x,\kappa) = \frac{6H(x-x_o)}{hh_o^3 E_o(\lambda_1^2-\lambda_2^2)(\lambda_2^2-\lambda_3^2)(\lambda_3^2-\lambda_1^2)} \sum_{j=1}^{3}\sum_{k=1}^{3}\sum_{\ell=1}^{3} \epsilon_{jk\ell}\,\lambda_k^2$$

$$\cdot\left\{A_1 \frac{1}{\lambda_j}\left[h\lambda_j^2 + \frac{2G(\kappa)}{h_o^2}\right]\sin\lambda_j(x-x_o) - A_2\left[\lambda_j^2 - \frac{2G(\kappa)}{h_o^2}\right]\cos\lambda_j(x-x_o)\right\}$$

$$\hat{\theta}_p(x,\kappa) = \frac{6H(x-x_o)}{hh_o^3 E_o(\lambda_1^2-\lambda_2^2)(\lambda_2^2-\lambda_3^2)(\lambda_3^2-\lambda_1^2)} \sum_{j=1}^{3}\sum_{k=1}^{3}\sum_{\ell=1}^{3} \epsilon_{jk\ell}\,\lambda_k^2 \qquad (5.7)$$

$$\cdot\left\{-A_1\left[\lambda_j^2 - \frac{2G(\kappa)}{h_o^2}\right]\cos\lambda_j(x-x_o) - A_2\left[\frac{4}{3h}\lambda_j^3 + \frac{2G(\kappa)}{h_o^2}\lambda_j\right.\right.$$

$$\left.\left. - \frac{2}{hh_o^2}(2+h\rho)\frac{\kappa^2}{c^2}\frac{1}{\lambda_j}\right]\sin\lambda_j(x-x_o)\right\}$$

$\epsilon_{jk\ell}$ are the components of the permutation tensor, and $H(x-x_o)$ is the unit step function, having the value 0 for $x < x_o$, and 1 for $x \geq x_o$. The solutions of the differential equations of (5.5) are the sums of the complementary functions and the particular solutions.

$$\begin{aligned}\hat{u}(x,\kappa) &= \hat{u}_c(x,\kappa) + \hat{u}_p(x,\kappa)\\ \hat{\theta}(x,\kappa) &= \hat{\theta}_c(x,\kappa) + \hat{\theta}_p(x,\kappa)\end{aligned} \qquad (5.8)$$

The six coefficients of (5.6), a_j, b_j (j = 1, 2, 3), are determined by applying the boundary conditions of (5.5) to (5.8). This

results in a system of six linear, algebraic equations

$$\mathcal{B}\underline{a} = \underline{\beta} \tag{5.9}$$

where $\underline{a}$ is a six element vector made up of the six coefficients, $\underline{\beta}$ is a six element vector, and $\mathcal{B}$ is a 6 x 6 matrix (see Appendix C). These coefficients can be evaluated using the theory of determinants.

Using the Fourier transform inversion formula (2.5), the solutions of (5.3) can be written as follows.

$$\begin{aligned} u(x,t) &= \frac{1}{2\pi}\int_{-\infty}^{\infty} \exp(i\kappa t)\,\hat{u}(x,\kappa)\,d\kappa \\ \theta(x,t) &= \frac{1}{2\pi}\int_{-\infty}^{\infty} \exp(i\kappa t)\,\hat{\theta}(x,\kappa)\,d\kappa \end{aligned} \tag{5.10}$$

If the shear relaxation modulus of the middle layer is represented as in (4.1), $\hat{u}(x,\kappa)$ and $\hat{\theta}(x,\kappa)$ will contain no branch points. Then it can be shown that the path of integration of (5.10) can be replaced by C_r, the closed contour of Fig. 4, in the limit as r becomes infinitely large. Therefore $u(x,t)$ and $\theta(x,t)$ can be evaluated by summing the residues of the integrands of (5.10) over the upper half of the complex frequency plane. Residues occur at points at which the integrands are singular. Consideration of (5.6) and (5.7) indicates that singularities arise due to two phenomena.

First, simple poles occur at the roots of the determinant, $\Delta(\kappa)$, of the matrix $\mathcal{B}$ of (5.9). (See (C.3) of Appendix C.) These enter (5.10) through the coefficients of the complementary functions (5.6). Singularities of this type would be present even if the shear relaxation modulus of the middle layer were a real, positive constant

(elastic three layer beam) rather than a monotonically decreasing function of time. In the elastic case the roots of the determinant would comprise an infinite set of positive-negative pairs of real numbers, whereas in the viscoelastic case these roots form an infinite set of pairs of complex numbers in which one is the negative complex conjugate of the other. Let those members of this infinite set which lie on the right side of the imaginary axis be labelled ω_n $(n = 1, 2, \ldots)$, where the subscripts are assigned in order of increasing distance from the origin. Then

$$\omega_n, \ -\bar{\omega}_n \qquad\qquad (n = 1, 2, \ldots)$$

where the bar $(\bar{\ })$ indicates complex conjugate, are all the members of the first set of singularities of the integrands of (5.10), and can be found from the condition

$$\Delta(\omega_n) = 0 \ .$$

The second set of singularities owes its existence to the presence of exponentially decaying terms in the shear relaxation modulus of the middle layer; it would not occur for an elastic beam. This set focuses on the N points $i\frac{1}{\tau_k}$ $(k = 1, 2, \ldots, N)$, where τ_k is the time constant of the kth exponentially decaying term. At each of these points the complex shear modulus (4.19) has a simple pole, which results in an essential singularity in $\hat{u}(x, \kappa)$ and $\hat{\theta}(x, \kappa)$. Each of these essential singularities is an accumulation point of an infinite sequence of simple poles, which lie on the imaginary axis

below the essential singularity. Let these simple poles be labelled $i\nu_{mn}$ $(m = 1, 2, \ldots, N;\ n = 1, 2, \ldots)$ where the first subscript identifies the sequence to which the simple pole belongs, and the second subscript identifies a particular member of the sequence, both indices being ordered according to increasing distance from the origin. Note that if the time constants are ordered such that $\tau_{k+1} > \tau_k$, then the mth sequence of simple poles has the accumulation point $i\frac{1}{\tau_{N+1-m}}$. These simple poles, as before, are points at which the determinant of β vanishes. Furthermore, by calculating λ_1, λ_2, λ_3 at the points $i\nu_{mn}$ and ω_n, for any m and n, it can be seen that the spatial functions associated with these two points are similar in shape, at least as far as having the same number of nodal points. Thus, each vibration mode of the beam is affected by contributions arising from N+2 eigenvalues; namely,

$$\omega_n,\ -\bar{\omega}_n,\ i\nu_{mn} \qquad (m = 1, 2, \ldots, N) \ .$$

Recall that in solving the simply-supported beam there were N+2 eigenvalues, related by (4.27), associated with each eigenfunction. Although in the present case one must settle for similar functions, rather than the same function, associated with a set of N+2 eigenvalues, the analogy between the two cases is apparent. Using the solution of the simply-supported beam as a guideline, it appears that the natural way to include the effects of the essential singularities in $u(x, t)$ and $\theta(x, t)$, is to consider separately the contribution of each simple pole of the sequence associated with each essential

singularity, and to allocate the contribution due to the pole $i\nu_{mn}$ to the vibration mode characterized by the natural frequency ω_n. This approach, although it increases the number of poles which must be found, allows the residue of every singularity in the upper half plane to be calculated by means of a single mathematical algorithm, since each singularity now has the property that it is a root of the determinant $\Delta(\kappa)$.

Before constructing the solutions $u(x, t)$ and $\theta(x, t)$, some observations on the solving of the algebraic system (5.9) may be useful. For the purpose of deciding at which points residues are to be calculated, it was assumed (5.9) was solved strictly according to the rules of determinant theory. An equivalent, but easier way to solve (5.9) is to solve first for the coefficients a_1, a_2, a_3. Then substitute these values back into (5.9), and choose any three of the four non-identically satisfied equations as a linear system involving b_1, b_2, b_3. This system need not be solved completely, since only those terms which contain $\Delta(\kappa)$ in the denominator contribute residues at the points ω_n, $-\bar{\omega}_n$, $i\nu_{mn}$ ($m = 1, 2, \ldots, N$; $n = 1, 2, \ldots$). Having solved (5.9), and having calculated the residues, (5.10) can be expressed as follows, where the functions employed are defined in (C.4), (C.5), (C.6), and (C.8) of Appendix C.

$$u(x,t) = \sum_{n=1}^{\infty} \left\{ 2\mathcal{R}\left[i \frac{A_1 W(x_o, \omega_n) - A_2 \Psi(x_o, \omega_n)}{E_o \Delta'(\omega_n)} \; U(x, \omega_n) \exp(i\omega_n t) \right] \right.$$

$$\left. + \sum_{m=1}^{N} \left[i \frac{A_1 W(x_o, i\nu_{mn}) - A_2 \Psi(x_o, i\nu_{mn})}{E_o \Delta'(i\nu_{mn})} \; U(x, i\nu_{mn}) \exp(-\nu_{mn} t) \right] \right\}$$

$$\theta(x,t) = \sum_{n=1}^{\infty} \left\{ 2\mathcal{R}\left[i \frac{A_1 W(x_o, \omega_n) - A_2 \Psi(x_o, \omega_n)}{E_o \Delta'(\omega_n)} \; \circledR\,(x, \omega_n) \exp(i\omega_n t) \right] \right. \tag{5.11}$$

$$\left. + \sum_{m=1}^{N} \left[i \frac{A_1 W(x_o, i\nu_{mn}) - A_2 \Psi(x_o, i\nu_{mn})}{E_o \Delta'(i\nu_{mn})} \; \circledR(x, i\nu_{mn}) \exp(-\nu_{mn} t) \right] \right\}$$

Using the above in the reciprocal identity (5.4), $w(x,t)$ and $\psi(x,t)$ can be expressed as follows, where $T(t,\kappa)$ is given by (C.7) of Appendix C.

$$w(x,t) = \sum_{n=1}^{\infty} \left\{ 2\mathcal{R}[W(x,\omega_n) T(t,\omega_n)] \right.$$

$$\left. + \sum_{m=1}^{N} [W(x, i\nu_{mn}) T(t, i\nu_{mn})] \right\}$$

$$\psi(x,t) = \sum_{n=1}^{\infty} \left\{ 2\mathcal{R}[\Psi(x,\omega_n) T(t,\omega_n)] \right. \tag{5.12}$$

$$\left. + \sum_{m=1}^{N} [\Psi(x, i\nu_{mn}) T(t, i\nu_{mn})] \right\}$$

The solution of the original boundary-initial value problem, i.e., (4.3), (4.5), (4.6), is obtained by way of the transformation (4.7).

$$v(x,t) = \sum_{j=1}^{6} g_{vj}(x) q_j(t) + \sum_{n=1}^{\infty} \left\{ 2\mathcal{R}\left[W(x,\omega_n) T(t,\omega_n) \right] + \sum_{m=1}^{N} \left[W(x, i\nu_{mn}) T(t, i\nu_{mn}) \right] \right\}$$

$$\varphi(x,t) = \sum_{j=1}^{6} g_{\varphi j}(x)\, q_j(t) + \sum_{n=1}^{\infty} \left\{ 2\mathcal{R}\left[\Psi(x,\omega_n) T(t,\omega_n) \right] + \sum_{m=1}^{N} \left[\Psi(x, i\nu_{mn}) T(t, i\nu_{mn}) \right] \right\} \qquad (5.13)$$

6. Calculations and Comparison with Experiment

A three-layer beam, for the purpose of checking the solution developed in Chapter 5, was constructed using two layers of aluminum and one layer of 50/50 Solithane 113. Of the boundary conditions which apply to the cantilever three-layer beam (5.1), the two most difficult to satisfy were B_2 and B_3, the slope of the beam at the fixed end. If these were both prescribed as zero, an effective way of satisfying these conditions experimentally would be to support the beam at midspan and load it symmetrically. Then because of symmetry, B_2 and B_3 would vanish at midspan. Thus midspan was considered to be the fixed end of a cantilever beam consisting of only half of the actual three-layer beam. Boundary conditions B_4, B_5, and B_6 of (5.1) were satisfied by prescribing them to be zero, and leaving the ends of the beam free. This left boundary condition B_1, the initial conditions $\underset{\sim}{y}(x)$ and $\underset{\sim}{\dot{y}}(x)$, and the transverse load $p(x, t)$ as the only remaining means of exciting the beam. In view of the requirement that the beam be loaded symmetrically, B_1 appeared to be the most practical of the choices available. Therefore $p(x, t)$, $\underset{\sim}{y}(x)$, and $\underset{\sim}{\dot{y}}(x)$ were all prescribed as zero, while $B_1[v(x, t), \varphi(x, t)]$, the transverse displacement of the fixed end, was prescribed as $q_1(t)$. Hence the experimental setup was described mathematically by the following boundary-initial value problem, in which L_j $(j = 1, 2)$ are defined by (4.2) and B_j $(j = 1, 2, \ldots, 6)$ are defined by (5.1).

$$
\begin{aligned}
&L_j[v(x,t),\varphi(x,t)] = 0 \qquad (j = 1,2)\\
&B_1[v(x,t),\varphi(x,t)] = q_1(t)\\
&B_j[v(x,t),\varphi(x,t)] = 0 \qquad (j = 2,3,\ldots,6)\\
&v(x,0) = 0, \qquad \dot{v}(x,0) = 0
\end{aligned}
\tag{6.1}
$$

Using these values of the boundary conditions, transverse loading, and initial conditions, along with (5.2), (4.9), and (4.11), the time dependence function (C.7) of Appendix C reduces to

$$
\begin{aligned}
T(t,\kappa) = i\,\frac{h_M\rho_M+2h_o\rho_o}{E_o\Delta'(\kappa)} \sum_{j=1}^{3}\sum_{k=1}^{3}\sum_{\ell=1}^{3} \epsilon_{jk\ell}\,\frac{\lambda_k}{\lambda_\ell^2}\\
\cdot\left[\frac{1-\cos\lambda_j L}{\lambda_j\cos\lambda_j L} - \frac{\sin\lambda_j L}{\lambda_j^2 C(\kappa)\cos\lambda_j L}\sum_{m=1}^{3}\lambda_m C_m(\kappa)\sin\lambda_m L\right]\\
\cdot\left\{\exp(i\kappa t)*\ddot{q}_1(t) + [i\kappa q_1(0)+\dot{q}_1(0)]\exp(i\kappa t)\right\}
\end{aligned}
\tag{6.2}
$$

where $C_m(\kappa)$ (m = 1, 2, 3) and $C(\kappa)$ are defined by (C.6).

The overall length of the three-layer beam was 36 inches. Therefore L, the length of one of the cantilever sections, was 18 inches. The width of the beam was 1 inch. The outer layers were aluminum of thickness h_o = 0.064 inches. The modulus of elasticity E_o and the specific weight of the outer layers were assumed to be 10^7 PSI and 0.098 lb/in^3, respectively. The middle layer was 50/50 Solithane 113, of thickness h_M = 0.032 inches. The specific weight of Solithane was taken as 0.036 lb/in^3. The shear modulus of 50/50 Solithane 113 is discussed in Appendix A. The temperature for which the calculations are applicable is 25° C. The governing equations

(6.1) call for the densities of the middle and outer layers, ρ_M, ρ_o, in units of lb · sec^2/in^4. To get these values, the specific weights were divided by 386.4.

Most of the difficulty encountered in applying the solution of Chapter 5 to a specific case was encountered while trying to find the eigenvalues ω_n, $i\nu_{mn}$ ($m = 1, 2, \ldots, N; n = 1, 2, \ldots$). The eigenvalues are roots of the equation

$$\Delta(\kappa) = 0 \tag{6.3}$$

where $\Delta(\kappa)$ is given by (C.3) of Appendix C. The technique employed to locate roots of (6.3) is an iterative one, based on Newton's method, in which the derivative of $\Delta(\kappa)$ is evaluated approximately by considering the difference in $\Delta(\kappa)$ at two neighboring values of κ. The resulting recursion formula is

$$\kappa_j = \kappa_{j-2} - \frac{(\kappa_{j-1}-\kappa_{j-2})\Delta(\kappa_{j-2})}{\Delta(\kappa_{j-1})-\Delta(\kappa_{j-2})} \tag{6.4}$$

where κ_j is the jth estimate of the eigenvalue to be found. This recursion formula (6.4) is similar to the one obtained in the method of false position (ref. 19).

This technique for finding eigenvalues requires the ability to calculate the value of $\Delta(\kappa)$ at some known value of κ. This was done by solving (4.23) using the exact formula for the roots of a cubic equation. This produced the values of λ_1, λ_2, λ_3 which were used

in (C. 3) to get $\Delta(\kappa)$. These calculations were executed on an IBM 370/155 computer, which has the limitation of not being able to accept a number larger than 7.237×10^{75}. Since numbers much larger than this were often encountered in the calculations, a system was devised whereby the magnitudes of many of the variables in the program were maintained between 1 and e^{50} by means of multiplying or dividing by e^{50} an appropriate number of times. Integer arrays were defined for the purpose of keeping track of the number of times a variable had been multiplied or divided by e^{50}, and several subroutines had to be written to supervise such operations as addition and finding the sine of a number with a large imaginary part.

Another requirement of the root finding scheme (6. 4) is an initial estimate of the root to be found. In fact (6. 4) requires two estimates. However, the second can be obtained from the first by choosing any point in the vicinity of the initial estimate, provided it is not so close that it satisfies the convergence criterion. The initial estimate of the complex eigenvalue ω_n was calculated, on the basis of the two previous complex eigenvalues, to be $2\omega_{n-1} - \omega_{n-2}$. In the case of ω_2, the initial estimate was $2\omega_1$. A satisfactory initial estimate of the first complex eigenvalue, ω_1, was found by considering a cantilever three-layer beam in which the shear modulus of the middle layer is infinitely large. The equations governing this problem were derived using the variational principle of Appendix B. The resulting boundary-initial value problem has the same form as that governing an elastic Bernoulli-Euler (ref. 20) cantilever beam, for which the first few natural frequencies are well known (ref. 21).

Thus the initial estimate of ω_1 was

$$\sqrt{\frac{c^2 h_o^2}{6(2+h\rho)}} \left(\frac{1.875}{L}\right)^2$$

In each of these cases the result of the iterative scheme (6.4) was accepted only if its value was relatively close to the initial estimate. This was to prevent the possibility of the iterative scheme converging to the wrong eigenvalue. In those cases for which the result was rejected, a new initial estimate was chosen.

Because of the close spacing of those eigenvalues which occur on the imaginary axis of the complex frequency plane, extremely accurate initial estimates were required. For this reason no automated system of generating initial estimates, such as that used for the complex eigenvalues, was found to be successful for the imaginary eigenvalues. Instead it was necessary to plot or list values of $\Delta(\omega)$ (C.3) along intervals of the imaginary axis, and to choose initial estimates according to changes in sign. If one of these initial estimates failed to produce the correct eigenvalue, a better initial estimate was obtained by plotting a smaller interval of the imaginary axis. This procedure eventually resulted in the set of eigenvalues $\omega_n, i\nu_{mn}$ ($m = 1, 2, \ldots, 8$; $n = 1, 2, \ldots, 12$) appearing in Table 1. Note that the sequence ν_{mn}, for each fixed value of m, tends toward a point of accumulation as described in Chapter 5. The values of the accumulation points are $3.935 \times 10^{m+2}$ ($m = 1, 2, \ldots, 8$).

Once the eigenvalues and the corresponding values of λ_1, λ_2, λ_3 were known, the evaluation of the eigenfunctions (C.5) and the time

dependence functions (6.2) was a matter of performing straightforward calculations, complicated slightly by the use of the e^{50} method mentioned above. One unexpected difficulty did arise, however. For many of the pure imaginary eigenvalues, λ_2 and λ_3 had real parts which were equal in magnitude to their imaginary parts for as many as eight significant figures. The calculation procedure called for subtraction of these nearly equal values. In order for the results of this subtraction to contain a reasonable number of significant figures, the entire computer program up to the point of this subtraction had to be written in double precision. But since the eigenvalues had been found by an iterative technique, accurate to within some error bound specified by the programmer, the accuracy of the result of the subtraction still had to be examined.

The subtraction associated with the imaginary eigenvalue for which m = 8, n = 1 was studied in detail. This is the case for which the real and imaginary parts of λ_2, λ_3 are most nearly equal. In this case

$$\lambda_2 = \lambda' + i\lambda'', \quad \lambda_3 = \lambda' - i\lambda''$$

$$\lambda' = 2.295566966021898 \times 10^3$$

$$\lambda'' = 2.295566960423937 \times 10^3$$

These values resulted from direct calculation based on the hypothesis that the corresponding eigenvalue was the number produced by the iterative technique, Z. Let the true eigenvalue be z. Then

$$z = Z(1 + \epsilon)$$

where ϵ is an unknown real number such that $|\epsilon|$ is less than the specified error bound of the iterative technique. The controversial subtraction occurred in the form

$$[\lambda_2(Z)]^2 + [\lambda_3(Z)]^2 = 2[(\lambda')^2 - (\lambda'')^2]$$

where the notation $\lambda_j(Z)$ (j = 2, 3) was used to emphasize the fact that λ_2, λ_3 were calculated based on the value Z for the associated eigenvalue. Analysis showed that, for m = 8, n = 1, the true value of this subtraction, based on the true eigenvalue z, would be

$$[\lambda_2(z)]^2 + [\lambda_3(z)]^2$$

$$= \left\{[\lambda_2(Z)]^2 + [\lambda_3(Z)]^2\right\}[1+4300\,\epsilon + O(|\epsilon|^2)]$$

Since the error bound of the iterative technique was specified to be 10^{-6}, the subtraction for this case was accurate to within 1%.

The time dependence of the only non-vanishing boundary condition (6.1), the transverse displacement of the beam at the fixed end, was chosen to be

$$q_1(t) = (1 - e^{-at}) \sin \omega t \qquad (6.5)$$

where $a = 10^{10}$ and ω is real. This function was chosen for two reasons. First, q(0) = 0 and $\dot{q}(0) = 0$. Thus there is no contradiction with the initial conditions, which state that the transverse displacement and the transverse velocity both vanish initially for

all points of the beam, including the fixed end. Second, because of the large value of a, $q_1(t)$ becomes indistinguishable from $\sin\omega t$, at least as far as the computer can tell, for all but extremely small values of t. Using (6.5) the time dependence function (6.2) becomes

$$T(t,\kappa) = i\,\frac{h_M\rho_M+2h_o\rho_o}{E_o\Delta'(\kappa)}\sum_{j=1}^{3}\sum_{k=1}^{3}\sum_{\ell=1}^{3}\epsilon_{jk\ell}\,\frac{\lambda_k}{\lambda_\ell^2}$$

$$\cdot\left[\frac{1-\cos\lambda_j L}{\lambda_j\cos\lambda_j L}-\frac{\sin\lambda_j L}{\lambda_j^2 C(\kappa)\cos\lambda_j L}\sum_{m=1}^{3}\lambda_m C_m(\kappa)\sin\lambda_m L\right]$$

$$\cdot\left\{\frac{\omega^2(i\kappa\sin\omega t+\omega\cos\omega t)}{\omega^2-\kappa^2}-\frac{\omega\kappa^2}{\omega^2-\kappa^2}\exp(i\kappa t)\right. \qquad (6.6)$$

$$+\frac{\omega\kappa^2}{\omega^2+(a+i\kappa)^2}\exp(i\kappa t)-\frac{(\omega^2-a^2)(a+i\kappa)-2a\omega^2}{\omega^2+(a+i\kappa)^2}\exp(-at)\sin\omega t$$

$$\left.-\left[1+\frac{\kappa^2}{\omega^2+(a+i\kappa)^2}\right]\omega\exp(-at)\cos\omega t\right\}$$

From this, the steady state time dependence may be obtained by neglecting every term which contains an exponential function.

The amplitude of the steady state transverse displacement at the free end of the beam was calculated from (5.13) for excitation frequencies up to 400 cycles per second. Since the amplitude of the displacement at the fixed end is 1, the results of this calculation can be presented in non-dimensional form as the ratio of the amplitude of the displacement at the free end to the amplitude of the displacement at the fixed end. This ratio has been plotted against

excitation frequency in Fig. 5. Five relative maxima of amplitude ratio response occur in the frequency interval of Fig. 5. These correspond, from left to right, respectively, to dominant influence in the response of the beam by the eigenfunction associated with ω_n $(n = 1, 2, \ldots, 5)$, the first five complex eigenvalues. The feature to be noticed in this figure is that for low excitation frequencies, the relative maxima in amplitude ratio response are large and sharply defined. But as the excitation frequency increases, the relative maxima become smaller and less sharply defined. The phenomenon of reduction in size and sharpness of a maximum in response has been attributed to increased damping in such well-known systems as the mass, spring, viscous damper (ref. 22). The amount of damping which belongs to any given eigenfunction of the viscoelastic three-layer beam problem depends on the imaginary part of the corresponding eigenvalue κ, through the terms $\exp(i\kappa t)$ appearing in (6.6). It is also the imaginary part of κ, since ω is real, which prevents the term

$$\frac{1}{\omega^2 - \kappa^2},$$

which also appears in (6.6), from becoming singular. It is primarily this latter term which accounts for the relative maxima in response, the size and sharpness of each maximum decreasing as the imaginary part of κ increases. Note that the values of the imaginary parts of ω_n $(n = 1, 2, \ldots, 5)$ listed in Table 1 increase while the maxima in response shown in Fig. 5 become smaller and broader. Thus, also

in the viscoelastic three-layer beam problem, increased damping reduces the size and sharpness of the relative maxima.

An experiment was performed in order to test the predictions of Fig. 5. The beam described at the beginning of this chapter was fastened to a shaker driven by a variable frequency oscillator through an amplifier (see Fig. 6). A counter was used to determine, with greater accuracy than the oscillator dials, the frequency of the input signal. The displacement of a point on the beam was measured using a reluctance pickup. Two voltage readings from the pickup were required in order to determine the displacement of the beam. A D. C. voltmeter was used to record the mean value of the pickup signal. This measurement was used to determine the distance from the pickup to the average position of the point on the beam. An oscilloscope was used to measure the variation of the pickup signal with respect to its mean value. This measurement was used to determine the amplitude of vibration at the point on the beam.

Measurements of this type were made at the fixed end of the cantilever beam; i. e., the point at which the double cantilever beam is fastened to the shaker, and at the four locations x = 4. 5", 9. 0", 13. 5", 18. 0". The last of the above locations is the free end of the beam. The amplitude of displacement ratio at each point was calculated by dividing the measured displacement amplitude at that point by the measured displacement amplitude at the fixed end. These ratios were measured for as large a frequency range as possible,

within the capability of the equipment used to record accurate, meaningful data. The accuracy of the displacement measurements declined rapidly as the amplitude of vibration fell below 0.005". Due to power limitations, displacement amplitudes large enough to allow sufficient accuracy could not be generated at higher frequencies. Furthermore, Fig. 5 indicates that the accessibility of meaningful data significantly declines as the frequency of excitation increases, due to the fact that the difference between maxima and minima of response decreases. In this experiment, the upper limit of availability of meaningful data occurred in the vicinity of 80 cycles per second.

The results of these measurements, for the four locations of the beam mentioned above, are plotted in Figs. 7, 8, 9, 10, along with curves of the theoretical amplitude ratio response. The theoretically and experimentally determined values agree in a number of respects. The maxima in response occur at approximately the same frequencies for both sets of data. The amplitudes of the response away from the maxima are approximately equal, and follow the same trends in both cases. And the width of the response peaks seems to be in agreement for the two cases. The area of most noticeable disagreement in Figs. 7, 8, 9, 10 is the amplitude of the response peaks, that feature which is most sensitive to the amount of damping associated with the dominant eigenfunction. In each case the theoretical values appear to be too high by approximately the same factor. One error which could affect the theoretical response in the manner described above would be to improperly

characterize the damping properties of the materials of the beam. The method used to characterize the shear modulus of Solithane 113 is outlined in Appendix A. The approximations used in this step, along with the fact that the nature of the discrepancy between theory and experiment is sensitive to damping, indicate that the most productive area in which to search for possible errors is likely to be the characterization of the shear modulus of the middle layer.

7. Summary

The response of a three-layer viscoelastic cantilever beam to steady state sinusoidal excitation was analyzed by solving the boundary-initial value problem (4.3), (4.5), (4.6) governing general dynamic response. This approach was considered to be superior, for reasons explained in Chapter 1, to that of applying the correspondence principle for sinusoidal oscillations[1], at least for the purpose of studying the response of the beam as a function of the frequency of excitation. This resulted in a solution characterized by a set of eigenvalues and eigenfunctions which are independent of the loading applied to the beam. Furthermore, the solution is applicable to cases other than steady state.

An experimental frequency response study was undertaken. The results of this study conformed to the predictions of the theoretical analysis in several respects. There was significant disagreement involving the amplitude of the response for frequencies in the neighborhood of the maxima in response.

---

[1] Bland, ref. 9, p. 67

REFERENCES

1. Plass, H. J., Jr., "Damping of Vibrations in Elastic Rods and Sandwich Structures by Incorporation of Additional Viscoelastic Material," Proceedings of the Third Midwestern Conference on Solid Mechanics (Ann Arbor, Mich.: University of Michigan Press, 1957), pp. 48-71.

2. Schwarzl, F., "Forced Bending and Extensional Vibrations of a Two-Layer Compound Linear Viscoelastic Beam," Acustica, Vol. 8 (1958), pp. 164-172.

3. Kerwin, Edward M., Jr., "Damping of Flexural Waves by a Constrained Viscoelastic Layer," The Journal of the Acoustical Society of America, Vol. 31 (1959), pp. 952-962.

4. Ross, Donald, Eric E. Ungar, and E. M. Kerwin, Jr., "Damping of Plate Flexural Vibrations by Means of Viscoelastic Laminae," Structural Damping, ed. Jerome E. Ruzicka (New York: ASME, 1959), pp. 49-87.

5. Yu, Yi-Yuan, "Damping of Flexural Vibrations of Sandwich Plates," Journal of the Aerospace Sciences, Vol. 29 (1962), pp. 790-803.

6. Di Taranto, R. A., "Theory of Vibratory Bending for Elastic and Viscoelastic Layered Finite-Length Beams," Journal of Applied Mechanics, Vol. 32 (1965), pp. 881-886.

7. Nicholas, T., "The Effects of Rotatory Inertia and Shear Deformation on the Flexural Vibrations of a Two-Layered Viscoelastic-Elastic Beam," Shock and Vibration Bulletin, (1968), pp. 13-28.

8. Kovac, Edward J., Jr., William J. Anderson, and Richard A. Scott, "Forced Non-linear Vibrations of a Damped Sandwich Beam," University of Michigan report, October 1970.

9. Bland, D. R., The Theory of Linear Viscoelasticity (New York: Pergamon Press, 1960).

10. Gurtin, M. E., and Eli Sternberg, "On the Linear Theory of Viscoelasticity," Archive for Rational Mechanics and Analysis, Vol. 11 (1962), pp. 291-356.

11. Gurtin, M. E., "Variational Principles for Linear Elastodynamics," Archive for Rational Mechanics and Analysis, Vol. 16 (1964), pp. 34-50.

12. Gurtin, M. E., "Variational Principles in the Linear Theory of Viscoelasticity," Archive for Rational Mechanics and Analysis, Vol. 13 (1963), pp. 179-191.

13. Libove, Charles, and S. B. Batdorf, "A General Small-Deflection Theory for Flat Sandwich Plates," NACA TN No. 1526 (April 1948).

14. Gerard, George, "Linear Bending Theory of Isotropic Sandwich Plates by an Order-of-Magnitude Analysis," Journal of Applied Mechanics, Vol. 19 (1952), pp. 13-15.

15. Cook, R. D., "On Certain Approximations in Sandwich Plate Analysis," Journal of Applied Mechanics, Vol. 33 (1966), pp. 39-44.

16. Mindlin, R. D., and L. E. Goodman, "Beam Vibrations With Time-Dependent Boundary Conditions," Journal of Applied Mechanics, Vol. 17 (1950), pp. 377-380.

17. Herrmann, G., "Forced Motions of Timoshenko Beams," Journal of Applied Mechanics, Vol. 22 (1955), pp. 53-56.

18. Yu, Yi-Yuan, "Forced Flexural Vibrations of Sandwich Plates in Plane Strain," Journal of Applied Mechanics, Vol. 27 (1960), pp. 535-540.

19. Isaacson, Eugene, and Herbert Bishop Keller, Analysis of Numerical Methods (New York: John Wiley & Sons, Inc., 1966).

20. Abramson, H. N., H. J. Plass, and E. A. Ripperger, "Stress Wave Propagation in Rods and Beams," Advances in Applied Mechanics, Vol. 5 (1958), pp. 111-194.

21. Timoshenko, S., Vibration Problems in Engineering (New York: D. Van Nostrand Company, Inc., 1937).

22. Tong, Kin N., Theory of Mechanical Vibrations (New York: John Wiley & Sons, Inc., 1960).

23. Knauss, W. G., J. F. Clauser, and R. F. Landel, "Second Report on the Selection of a Cross-Linked Polymer Standard," AFRPL-TR-66-21.

24. Ferry, John D., Viscoelastic Properties of Polymers (New York: John Wiley & Sons, Inc., 1961).

Appendix A

Exponential Series Representation of the Shear Modulus of 50/50 Solithane 113

Let G_m (m = 1, 2, . . . , M) be a set of M known values of the complex shear modulus, each valid at some real value of frequency, $\tilde{\omega}_m$. It is the purpose of this appendix to find a function of the form

$$\mu(t) = \mu_E + \sum_{n=1}^{N} \mu_n \exp(-t/\tau_n), \qquad t > 0 \tag{A. 1}$$

such that its complex modulus form

$$\tilde{\mu}(\omega) = \mu(0) - \sum_{n=1}^{N} \frac{\mu_n}{1+i\omega\tau_n}, \quad \mu(0) = \mu_E + \sum_{n=1}^{N} \mu_n \tag{A. 2}$$

takes on values sufficiently close to the known values of the complex shear modulus at the appropriate frequencies. No suggestion will be made here as to how closely (A. 2) and the known values must agree in order that (A. 1) should be considered an acceptable approximation of the true shear modulus. This value judgement should be left up to the individual user of the approximation, who should be warned that better agreement will, most likely, require a larger value of N, which, in turn, will very often increase the complexity of the problem he wishes to solve.

Let the difference between (A. 2) and the known values of the complex shear modulus be quantified by means of the function

$$\mathcal{E} = \sum_{m=1}^{M} \left| G_m - \tilde{\mu}(\tilde{\omega}_m) \right|^2 \tag{A. 3}$$

Then the values of the parameters of (A. 2) can be determined by minimizing $\mathcal{E}$ with respect to each parameter, and solving the

resulting system of equations. If rather than determining all the parameters in this manner, one chooses the time constants in advance, and minimizes $\mathcal{E}$ with respect to only the coefficients $\mu(0)$, μ_n $(n = 1, 2, \ldots, N)$, the resulting algebraic system is linear. Let

$$\mu_o = -\mu(0), \quad \tau_o = 0 \tag{A.4}$$

Then, setting

$$\frac{\partial \mathcal{E}}{\partial \mu_k} = 0 \qquad (k = 0, 1, \ldots, N)$$

results in the following system of (N+1) equations.

$$\sum_{n=0}^{N} \mu_n \sum_{m=1}^{M} \frac{\mathcal{R}\left\{\frac{1+i\tilde{\omega}_m \tau_k}{1+i\tilde{\omega}_m \tau_n}\right\}}{1+\tilde{\omega}_m^2 \tau_k^2} = -\sum_{m=1}^{M} \frac{\mathcal{R}\{G_m(1+i\tilde{\omega}_m \tau_k)\}}{1+\tilde{\omega}_m^2 \tau_k^2} \tag{A.5}$$

$$(k = 0, 1, \ldots, N)$$

This set of equations can be solved by matrix methods to determine the (N+1) unknowns μ_n $(n = 0, 1, \ldots, N)$.

Knauss, Clauser, and Landel (ref. 23) have published curves of the complex Young's modulus of various compositions of Solithane 113.[1] The complex shear modulus and the complex Young's modulus of a material are related by the expression

---

[1] Although the reference temperature is given as 20°C in ref. 23, comparison with other data available at Caltech indicates that, at least for 50/50 Solithane 113, 0°C is the correct reference temperature for these curves.

$$\tilde{\mu}(\omega) = \frac{\tilde{E}(\omega)}{2[1+\tilde{\nu}(\omega)]}$$

where $\tilde{\nu}(\omega)$ is the complex Poisson's ratio. In the absence of a curve of the complex shear modulus, $\tilde{\nu}(\omega)$ was assigned the value $\frac{1}{2}$ so that "known values" of the complex shear modulus could be deduced from the curves in ref. 23.

Ninety-one points, ranging from $\omega = 0.1$ cps to $\omega = 10^8$ cps, were read from the curves in ref. 23 to be used in (A. 5). Using the eight time constants

$$\tau_n = 10^{(n-8)} \text{ sec } (n = 1, 2, \ldots, 8)$$

the coefficients shown in Table 2 were obtained. Fig. 11 compares (A. 2), using the coefficients of Table 2, with the input values of the complex shear modulus. Fig. 11 shows only every fifth input value. The comparison shows that for any given frequency, (A. 2) produces a value which is not very different from the actual complex shear modulus for that frequency. However, one can detect from Fig. 11 an oscillatory behavior of (A. 2) which is not present in the input values. A discrete spectrum of time constants will always produce such oscillations. If these oscillations are objectionable, their amplitudes can be reduced by choosing more time constants spaced closer together on the logarithmic time axis; and they can be eliminated by considering a continuous spectrum of time constants. Fig. 12 compares (A. 2), using the coefficients of Table 3, with the input values. Note that the oscillations are no longer perceptible. It was decided that, for the purpose of this

paper, sizable oscillations in the complex shear modulus representation could be tolerated with much less difficulty than an excessive number of time constants. Therefore the values of Table 2 were chosen for use throughout this paper.

The values of Table 2 form a valid representation of the complex shear modulus of 50/50 Solithane 113, only at the temperature 0° C. For temperatures other than 0° C, the complex shear modulus takes the form

$$\tilde{\mu}(\omega) = \frac{T+273}{273} \left[\mu(0) - \sum_{n=1}^{N} \frac{\mu_n}{1+i\omega a_T \tau_n} \right] \qquad (A.6)$$

where T is the temperature in degrees, Centigrade, and a_T is the time-temperature shift factor. A set of experimentally determined values of a_T, plotted as a function of T, was fitted to the WLF equation (see Ferry, ref. 24) with the intention of getting the best possible fit in the neighborhood of average room temperature of the laboratory (25° C). The following expression was obtained.

$$\log_{10}(a_T) = - \frac{13.316T}{67.6+T} \qquad (A.7)$$

Appendix B

A Variational Principle for Dynamic Motion of a Linearly Viscoelastic Body

Let R be the region of space occupied by a viscoelastic body, and let B be the boundary of R. Let B_1 be the portion of B on which displacement boundary conditions are prescribed; and B_2, the portion on which traction boundary conditions are prescribed. Let the prescribed value of the displacement vector on B_1 be $\underline{\mathring{u}}(\underline{x}, t)$, and let the prescribed value of the traction vector on B_2 be $\underline{\mathring{s}}(\underline{x}, t)$. Let $\underline{F}(\underline{x}, t)$ be the body force field on R; and let $\underline{G}(\underline{x}, t)$, a fourth order tensor function with the symmetry properties

$$G_{ijk\ell}(\underline{x}, t) = G_{jik\ell}(\underline{x}, t) = G_{k\ell ij}(\underline{x}, t) , \tag{B. 1}$$

be the relaxation modulus tensor of the material, relating stress and strain as follows.

$$\sigma_{ij}(\underline{x}, t) = \gamma_{k\ell}(\underline{x}, t) * dG_{ijk\ell}(\underline{x}, t) \tag{B. 2}$$

The relationship (B. 2) is, in general, anisotropic and inhomogeneous. An isotropic material has a relaxation modulus tensor with components

$$G_{ijk\ell}(\underline{x}, t) = \frac{1}{3}\delta_{ij}\delta_{k\ell}[3K(\underline{x}, t) - 2\mu(\underline{x}, t)] + (\delta_{ik}\delta_{j\ell} + \delta_{i\ell}\delta_{jk})\mu(\underline{x}, t) \tag{B. 3}$$

where δ_{ij} are the components of the Kronecker delta. Thus, an isotropic material meets the symmetry relations (B. 1).

Let the initial displacement vector be $\underline{d}(\underline{x})$, and the initial velocity vector be $\underline{v}(\underline{x})$. Thus, the prescribed initial conditions are

$$\underline{u}(\underline{x}, 0) = \underline{d}(\underline{x}), \qquad \dot{\underline{u}}(\underline{x}, 0) = \underline{v}(\underline{x}) \tag{B.4}$$

where, in the case of discontinuous displacement histories, $\underline{u}(\underline{x}, 0)$ and $\dot{\underline{u}}(\underline{x}, 0)$ are the limits of $\underline{u}(\underline{x}, t)$ and $\dot{\underline{u}}(\underline{x}, t)$, respectively, as t approaches 0 through positive values. Let the symbol $g(t)$ be used to denote the function

$$\begin{aligned} g(t) &= 0 \qquad (-\infty < t < 0) \\ g(t) &= \tfrac{1}{2}t^2 \quad (0 \leqslant t < \infty) \end{aligned} \tag{B.5}$$

and let the symbol $\underline{f}(\underline{x}, t)$ denote the vector function with the components

$$f_i(\underline{x}, t) = F_i(\underline{x}, t) * dg(t) + \rho(\underline{x})[tv_i(\underline{x}) + d_i(\underline{x})] \tag{B.6}$$

where $\rho(\underline{x})$ is the density of the body at point $\underline{x}$.

Let A be the set of all kinematically admissible states, as defined by Gurtin (ref. 11). Briefly, a state

$$S = [\underline{u}(\underline{x}, t), \ \underline{\gamma}(\underline{x}, t), \ \underline{\sigma}(\underline{x}, t)]$$

is an ordered combination of vector and tensor functions $\underline{u}$, $\underline{\gamma}$, $\underline{\sigma}$ which represent, respectively, the displacement vector, the strain tensor, and the stress tensor. A kinematically admissible state is a state which satisfies in addition to some lenient smoothness conditions specified in ref. 11, the strain-displacement relations,

$$\gamma_{ij}(\underline{x}, t) = \tfrac{1}{2}[u_{i,j}(\underline{x}, t) + u_{j,i}(\underline{x}, t)] \qquad \text{(B. 7)}$$

the stress-strain relations (B. 1, B. 2), and the displacement boundary conditions

$$\underline{u}(\underline{x}, t) = \overset{\circ}{\underline{u}}(\underline{x}, t) \text{ for } \underline{x} \text{ on } B_1. \qquad \text{(B. 8)}$$

Let the variation of a functional over A, the set of all kinematically admissible states, be defined as (see ref. 11, 12)

$$\delta\Omega\{S\} = \frac{d}{d\zeta}\Omega\{S+\zeta(\delta S)\}\Big|_{\zeta=0}$$

for S and $[S+\zeta(\delta S)]$ in A

Define the functional $\Phi\{S\}$, for all S in A, as

$$\begin{aligned}\Phi\{S\} = {} & \tfrac{1}{2}\int_R g(t)*d\sigma_{ij}(\underline{x}, t)*d\gamma_{ij}(\underline{x}, t)\,d\underline{x} \\ & + \tfrac{1}{2}\int_R \rho(\underline{x})u_i(\underline{x}, t)*du_i(\underline{x}, t)d\underline{x} \\ & - \int_R f_i(\underline{x}, t)*du_i(\underline{x}, t)d\underline{x} \\ & - \int_{B_2} g(t)*d\overset{\circ}{s}_i(\underline{x}, t)*du_i(\underline{x}, t)d\underline{x}\end{aligned} \qquad \text{(B. 9)}$$

where the symbol $d\underline{x}$ represents an infinitesimal element of either surface or volume, depending on the region of integration specified below the integration symbol. Then for every kinematically admissible state (i. e., S in A), the relation

$$\delta\Phi\{S\} = 0 \qquad \text{(B. 10)}$$

holds if, and only if, the following relations hold:

$$\sigma_{ij,\,j}(\underline{x}, t) + F_i(\underline{x}, t) = \rho(\underline{x})\ddot{u}_i(\underline{x}, t) \text{ in } R$$

$$\sigma_{ij}(\underline{x}, t)n_j(\underline{x}) = \mathring{s}_i(\underline{x}, t) \text{ on } B_2 \qquad \text{(B. 11)}$$

$$\underline{u}(\underline{x}, 0) = \underline{d}(\underline{x}),\ \dot{\underline{u}}(\underline{x}, 0) = \underline{v}(\underline{x}) \text{ in } R$$

where $n_j(\underline{x})$ are the components of the outward unit normal vector to the boundary B at point $\underline{x}$. The above, together with the relations which, by definition, must hold for a kinematically admissible state, completely define the boundary-initial value problem under consideration. Thus (B. 10) must give the state which is the solution to that problem.

To prove this variational principle, take the variation of $\Phi\{S\}$ (B. 9). Using the stress-strain relations, the strain-displacement relations, and the displacement boundary conditions, all of which must hold since S is in A; and making use of the properties of the Stieltjes convolution (see ref. 10) and the divergence theorem, one gets

$$\begin{aligned}\delta\Phi\{S\} = \int_R [&-g(t)*d\sigma_{ij,\,j}(\underline{x}, t) + \rho(\underline{x})u_i(\underline{x}, t) \\ &-f_i(\underline{x}, t)] *d\delta u_i(\underline{x}, t)d\underline{x} \\ &+\int_{B_2} g(t)*d[\sigma_{ij}(\underline{x}, t)n_j(\underline{x}) - \mathring{s}_i(\underline{x}, t)] \\ &*d\delta u_i(\underline{x}, t)d\underline{x}\end{aligned} \qquad \text{(B. 12)}$$

First, let (B. 11) hold. Using (B. 11) and (B. 6) in (B. 12), one gets

$$\delta\Phi\{S\} = \int_R \rho(\underline{x}) [u_i(\underline{x}, t) - t\, v_i(\underline{x}) - d_i(\underline{x})$$

$$-g(t)*d\mathring{u}_i(\underline{x}, t)] *d\delta u_i(\underline{x}, t)d\underline{x}$$

It can be shown, through integration by parts, that for any function $\varphi(\underline{x}, t)$, and for g(t) as defined in (B. 5), the following identity holds.

$$g(t)*d\ddot{\varphi}(\underline{x}, t) = \varphi(\underline{x}, t) - \varphi(\underline{x}, 0) - t\dot{\varphi}(\underline{x}, 0)$$

This, and the initial conditions of (B. 11) give (B. 10).

Next, let (B. 10) hold. This and (B. 12), together with the fact that $\delta u_i(\underline{x}, t)$ can be chosen arbitrarily within the limitation that $S + \lambda\delta S$ must be a member of A, imply the following.

$$\begin{aligned} -g(t)*d\sigma_{ij,j}(\underline{x}, t)+\rho(\underline{x})u_i(\underline{x}, t)-f_i(\underline{x}, t) &= 0 \text{ in } R \\ g(t)*d[\sigma_{ij}(\underline{x}, t)n_j(\underline{x})-\mathring{s}_i(\underline{x}, t)] &= 0 \text{ on } B_2 \end{aligned} \qquad \text{(B. 13)}$$

The property of the Stieltjes convolution (see ref. 10) that

$$\varphi(t)*d\psi(t) = 0$$

implies either $\varphi(t) \equiv 0$ or $\psi(t) \equiv 0$, and the fact that g(t) does not vanish identically (B. 5), immediately verifies the second of (B. 11). Using (B. 5) and (B. 6), the first of (B. 13) can be rewritten as

$$-\int_0^t (t-\tau)[\sigma_{ij,j}(\underline{x}, \tau) + F_i(\underline{x}, \tau)]\, d\tau$$

$$+\rho(\underline{x})[u_i(\underline{x}, t)-tv_i(\underline{x})-d_i(\underline{x})] = 0 \text{ in } R \ .$$

Setting t = 0 implies

$$u_i(\underline{x}, 0) = d_i(\underline{x}) .$$

Now differentiate with respect to t, to get

$$-\int_0^t [\sigma_{ij,j}(\underline{x}, \tau)+F_i(\underline{x}, \tau)]\, d\tau$$

$$+\rho(\underline{x})[\dot{u}_i(\underline{x}, t)-v_i(\underline{x})] = 0 \quad \text{in } R.$$

Setting t = 0 implies

$$\dot{u}_i(\underline{x}, 0) = v_i(\underline{x}) .$$

Thus, the third of (B. 11) holds. Differentiating again with respect to t verifies the first of (B. 11). This completes the proof.

Appendix C

(C.1)

$$
\underline{\alpha} = \begin{Bmatrix} a_1 \\ b_1 \\ a_2 \\ b_2 \\ a_3 \\ b_3 \end{Bmatrix} \qquad \underline{\beta} = \begin{Bmatrix}
0 \\
0 \\
0 \\
\dfrac{6}{hh_o^3 E_o(\lambda_1^2-\lambda_2^2)(\lambda_2^2-\lambda_3^2)(\lambda_3^2-\lambda_1^2)} \sum_{j=1}^{3}\sum_{k=1}^{3}\sum_{\ell=1}^{3} \epsilon_{jk\ell}\lambda_k^2 \\
\cdot\left\{-A_1\dfrac{1}{\lambda_j}\dfrac{1}{2}\left[h\lambda_j^2+\dfrac{2G(\kappa)}{h_o^2}\right]\cos\lambda_j(L-x_o)+A_2\dfrac{1}{\lambda_j}\left[\lambda_j^2-\dfrac{2G(\kappa)}{h_o^2}\right]\sin\lambda_j(L-x_o)\right\} \\
\dfrac{6}{hh_o^3 E_o(\lambda_1^2-\lambda_2^2)(\lambda_2^2-\lambda_3^2)(\lambda_3^2-\lambda_1^2)} \sum_{j=1}^{3}\sum_{k=1}^{3}\sum_{\ell=1}^{3} \epsilon_{jk\ell}\lambda_k^2 \\
\cdot\left\{-A_1\lambda_j\left[h\lambda_j^2+\dfrac{2G(\kappa)}{h_o^2}\right]\sin\lambda_j(L-x_o)-A_2\lambda_j^2\left[\lambda_j^2-\dfrac{2G(\kappa)}{h_o^2}\right]\cos\lambda_j(L-x_o)\right\} \\
\dfrac{6}{hh_o^3 E_o(\lambda_1^2-\lambda_2^2)(\lambda_2^2-\lambda_3^2)(\lambda_3^2-\lambda_1^2)} \sum_{j=1}^{3}\sum_{k=1}^{3}\sum_{\ell=1}^{3} \epsilon_{jk\ell}\lambda_k^2 \\
\cdot\left\{-A_1\dfrac{1}{\lambda_j^3}\left[h\lambda_j^2+\dfrac{2G(\kappa)}{h_o^2}\right]\sin\lambda_j(L-x_o)-A_2\dfrac{1}{\lambda_j^2}\left[\lambda_j^2-\dfrac{2G(\kappa)}{h_o^2}\right]\cos\lambda_j(L-x_o)\right\}
\end{Bmatrix}
$$

$$\mathcal{B} = \begin{pmatrix} 0 & 1 & 0 & 1 & 0 & 1 \\ \lambda_1 & 0 & \lambda_2 & 0 & \lambda_3 & 0 \\ \frac{1}{\lambda_1^3} & 0 & \frac{1}{\lambda_2^3} & 0 & \frac{1}{\lambda_3^3} & 0 \\ \frac{1}{\lambda_1}\cos\lambda_1 L & -\frac{1}{\lambda_1}\sin\lambda_1 L & \frac{1}{\lambda_2}\cos\lambda_2 L & -\frac{1}{\lambda_2}\sin\lambda_2 L & \frac{1}{\lambda_3}\cos\lambda_3 L & -\frac{1}{\lambda_3}\sin\lambda_3 L \\ \lambda_1^2 \sin\lambda_1 L & \lambda_1^2 \cos\lambda_1 L & \lambda_2^2 \sin\lambda_2 L & \lambda_2^2 \cos\lambda_2 L & \lambda_3^2 \sin\lambda_3 L & \lambda_3^2 \cos\lambda_3 L \\ \frac{1}{\lambda_1^2}\sin\lambda_1 L & \frac{1}{\lambda_1^2}\cos\lambda_1 L & \frac{1}{\lambda_2^2}\sin\lambda_2 L & \frac{1}{\lambda_2^2}\cos\lambda_2 L & \frac{1}{\lambda_3^2}\sin\lambda_3 L & \frac{1}{\lambda_3^2}\cos\lambda_3 L \end{pmatrix}$$

(C. 2)

$$\Delta(\kappa) = \frac{1}{\lambda_1\lambda_2\lambda_3}\left\{2\left[\frac{\lambda_2^2}{\lambda_3^2}+\frac{\lambda_3^2}{\lambda_2^2}-\frac{\lambda_1^4}{\lambda_2^2\lambda_3^2}-\frac{\lambda_2^2\lambda_3^2}{\lambda_1^4}\right]\cos\lambda_1 L\right.$$

$$+2\left[\frac{\lambda_3^2}{\lambda_1^2}+\frac{\lambda_1^2}{\lambda_3^2}-\frac{\lambda_2^4}{\lambda_3^2\lambda_1^2}-\frac{\lambda_3^2\lambda_1^2}{\lambda_2^4}\right]\cos\lambda_2 L$$

$$+2\left[\frac{\lambda_1^2}{\lambda_2^2}+\frac{\lambda_2^2}{\lambda_1^2}-\frac{\lambda_3^4}{\lambda_1^2\lambda_2^2}-\frac{\lambda_1^2\lambda_2^2}{\lambda_3^4}\right]\cos\lambda_3 L$$

$$+\left[\frac{\lambda_1^4}{\lambda_2^4}+\frac{\lambda_2^4}{\lambda_3^4}+\frac{\lambda_3^4}{\lambda_1^4}+\frac{\lambda_2^4}{\lambda_1^4}+\frac{\lambda_3^4}{\lambda_2^4}+\frac{\lambda_1^4}{\lambda_3^4}-6\right]$$

$$\cdot\cos\lambda_1 L\cos\lambda_2 L\cos\lambda_3 L \qquad \text{(C. 3)}$$

$$+\left[\frac{\lambda_1^4}{\lambda_2^3\lambda_3}+\frac{\lambda_2^3\lambda_3}{\lambda_1^4}+\frac{\lambda_1^4}{\lambda_2\lambda_3^3}+\frac{\lambda_2\lambda_3^3}{\lambda_1^4}-\frac{\lambda_2}{\lambda_3}-\frac{\lambda_3}{\lambda_2}-\frac{\lambda_2^3}{\lambda_2^3}-\frac{\lambda_3^3}{\lambda_2^3}\right]$$

$$\cdot\cos\lambda_1 L\sin\lambda_2 L\sin\lambda_3 L$$

$$+\left[\frac{\lambda_2^4}{\lambda_3^3\lambda_1}+\frac{\lambda_3^3\lambda_1}{\lambda_2^4}+\frac{\lambda_2^4}{\lambda_3\lambda_1^3}+\frac{\lambda_3\lambda_1^3}{\lambda_2^4}-\frac{\lambda_3}{\lambda_1}-\frac{\lambda_1}{\lambda_3}-\frac{\lambda_3^3}{\lambda_1^3}-\frac{\lambda_1^3}{\lambda_3^3}\right]$$

$$\cdot\cos\lambda_2 L\sin\lambda_3 L\sin\lambda_1 L$$

$$+\left[\frac{\lambda_3^4}{\lambda_1^3\lambda_2}+\frac{\lambda_1^3\lambda_2}{\lambda_3^4}+\frac{\lambda_3^4}{\lambda_1\lambda_2^3}+\frac{\lambda_1\lambda_2^3}{\lambda_3^4}-\frac{\lambda_1}{\lambda_2}-\frac{\lambda_2}{\lambda_1}-\frac{\lambda_1^3}{\lambda_2^3}-\frac{\lambda_2^3}{\lambda_1^3}\right]$$

$$\left.\cdot\cos\lambda_3 L\sin\lambda_1 L\sin\lambda_2 L\right\}$$

$$U(x,\kappa) = \sum_{j=1}^{3}\sum_{k=1}^{3}\sum_{\ell=1}^{3} \epsilon_{jk\ell}\,\frac{\lambda_k}{\lambda_\ell^3}\left[-\frac{\sin\lambda_j(L-x)}{\cos\lambda_j L} + \frac{\cos\lambda_j x}{C(\kappa)\lambda_j\cos\lambda_j L}\sum_{m=1}^{3}\lambda_m C_m(\kappa)\sin\lambda_m L\right]$$

$$\Theta(x,\kappa) = \sum_{j=1}^{3}\sum_{k=1}^{3}\sum_{\ell=1}^{3} \epsilon_{jk\ell}\,\frac{\lambda_k}{\lambda_\ell^3}\,\frac{\lambda_j^2 - \frac{2G(\kappa)}{h_o^2}}{h\lambda_j^2 + \frac{2G(\kappa)}{h_o^2}}\left[-\frac{\lambda_j\cos\lambda_j(L-x)}{\cos\lambda_j L} + \frac{\sin\lambda_j x}{C(\kappa)\cos\lambda_j L}\sum_{m=1}^{3}\lambda_m C_m(\kappa)\sin\lambda_m L\right] \qquad (C.4)$$

$$W(x,\kappa) = -\frac{6}{hh_o^3(\lambda_1^2-\lambda_2^2)(\lambda_2^2-\lambda_3^2)(\lambda_3^2-\lambda_1^2)} \cdot \sum_{j=1}^{3}\sum_{k=1}^{3}\sum_{\ell=1}^{3} \epsilon_{jk\ell}\,\lambda_k^2\left[h\lambda_j^2 + \frac{2G(\kappa)}{h_o^2}\right]\left[\frac{C(\kappa)\cos\lambda_j x}{\lambda_j^2\cos\lambda_j L} - \frac{\sin\lambda_j(L-x)}{\lambda_j\cos\lambda_j L}\sum_{m=1}^{3}\frac{C_m(\kappa)\sin\lambda_m L}{\lambda_m}\right] \qquad (C.5)$$

$$\Psi(x,\kappa) = -\frac{6}{hh_o^3(\lambda_1^2-\lambda_2^2)(\lambda_2^2-\lambda_3^2)(\lambda_3^2-\lambda_1^2)} \cdot \sum_{j=1}^{3}\sum_{k=1}^{3}\sum_{\ell=1}^{3} \epsilon_{jk\ell}\,\lambda_k^2\left[\lambda_j^2 - \frac{2G(\kappa)}{h_o^2}\right]\left[\frac{C(\kappa)\sin\lambda_j x}{\lambda_j\cos\lambda_j L} - \frac{\cos\lambda_j(L-x)}{\cos\lambda_j L}\sum_{m=1}^{3}\frac{C_m(\kappa)\sin\lambda_m L}{\lambda_m}\right]$$

$$C_j(\kappa) = \sum_{k=1}^{3} \sum_{\ell=1}^{3} \epsilon_{jk\ell} \frac{\lambda_k^2}{\lambda_\ell^2} \cos\lambda_k L \cos\lambda_\ell L$$

$$C(\kappa) = \sum_{j=1}^{3} C_j(\kappa) \qquad \text{(C. 6)}$$

$$T(t, \kappa) = i \frac{1}{E_o \Delta'(\kappa)} \left\{ \exp(i\kappa t) * \int_0^L [U(\xi, \kappa) P_1(\xi, t) \right.$$

$$- \Theta(\xi, \kappa) P_2(\xi, t)] \, d\xi + (h_M \rho_M + 2h_o \rho_o) \exp(i\kappa t) \qquad \text{(C. 7)}$$

$$\left. \cdot \int_0^L [i\kappa \underset{\sim}{w}(\xi) + \dot{\underset{\sim}{w}}(\xi)] \, U(\xi, \kappa) d\xi \right\}$$

$$\Delta'(\kappa) = \frac{d}{d\kappa} \Delta(\kappa) \qquad \text{(C. 8)}$$

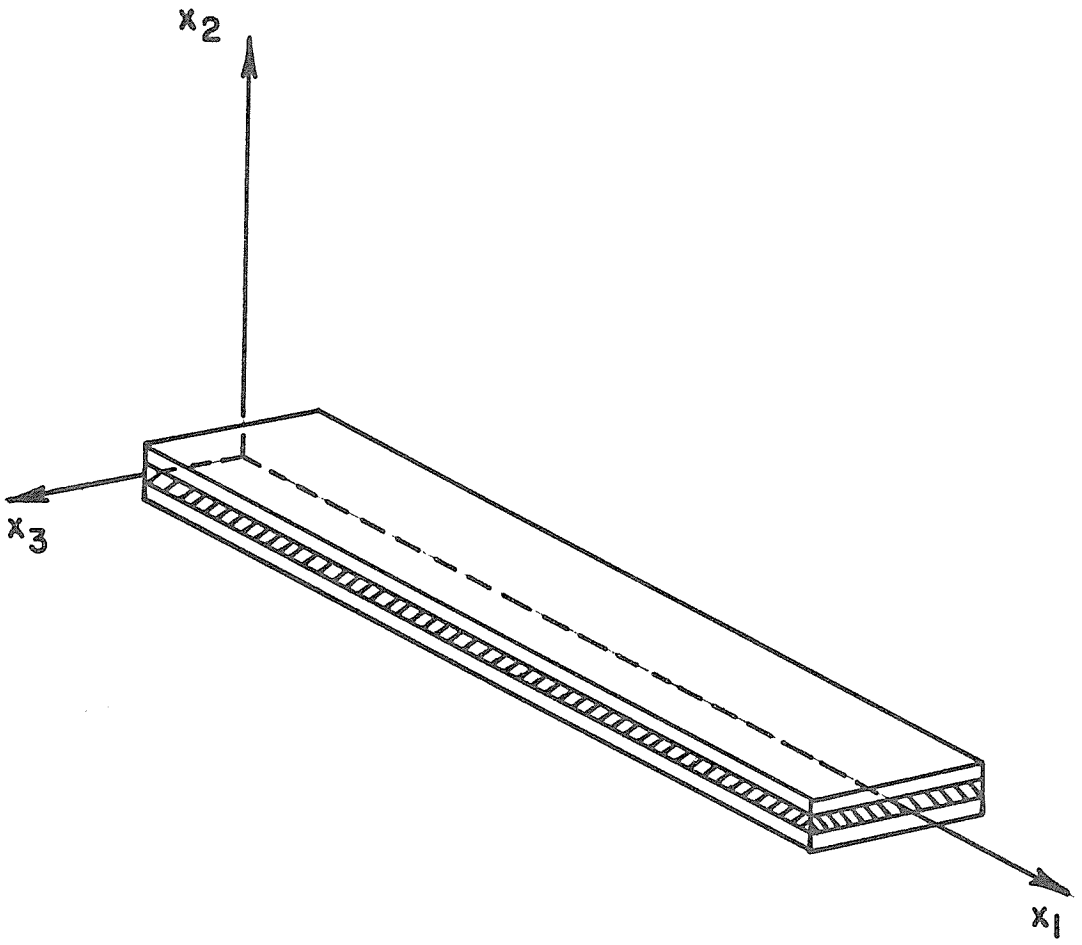

FIG. 1 THREE-LAYER BEAM IN x_1, x_2, x_3 COORDINATE SYSTEM

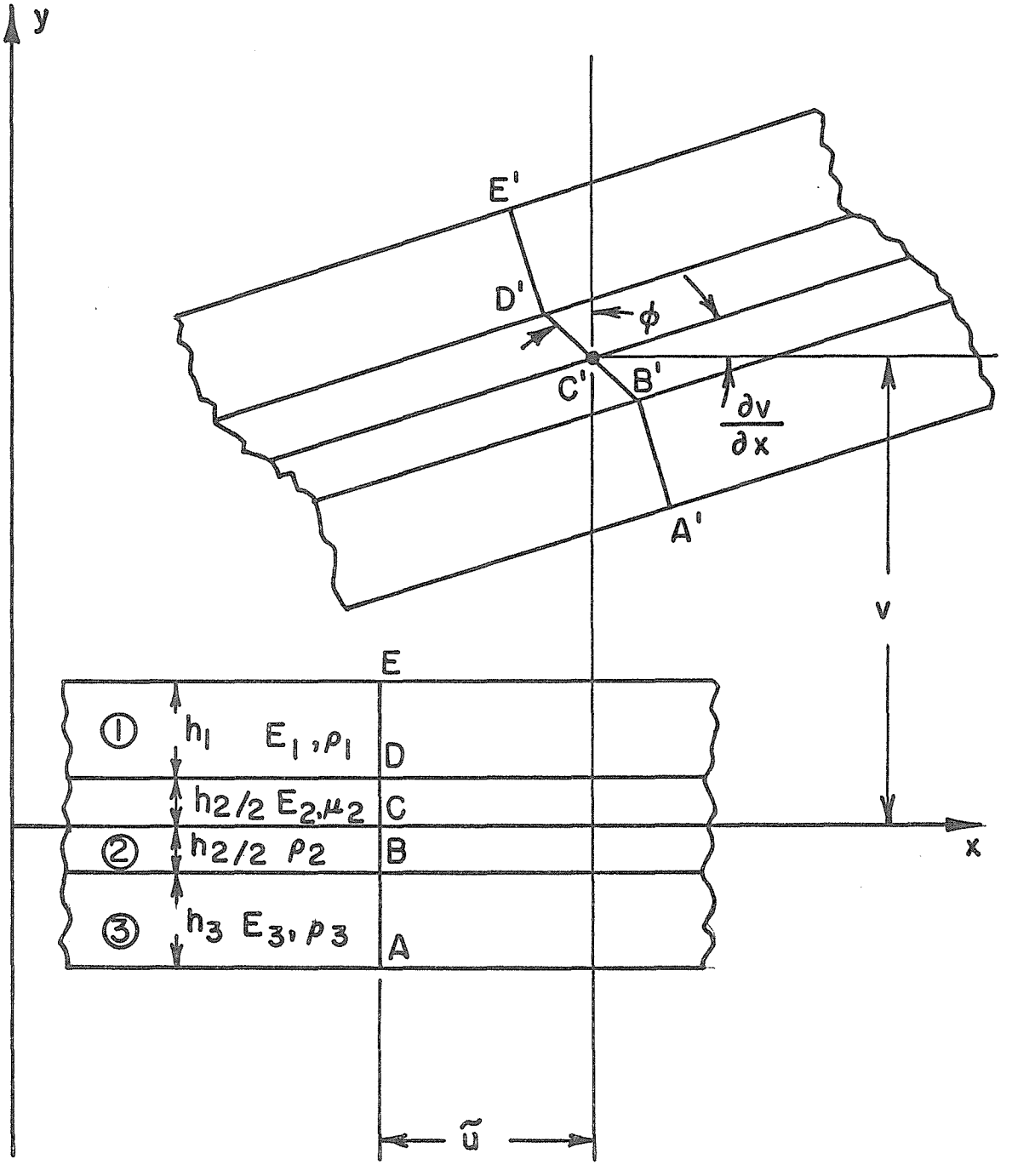

FIG. 2 DISPLACEMENT OF A BEAM ELEMENT

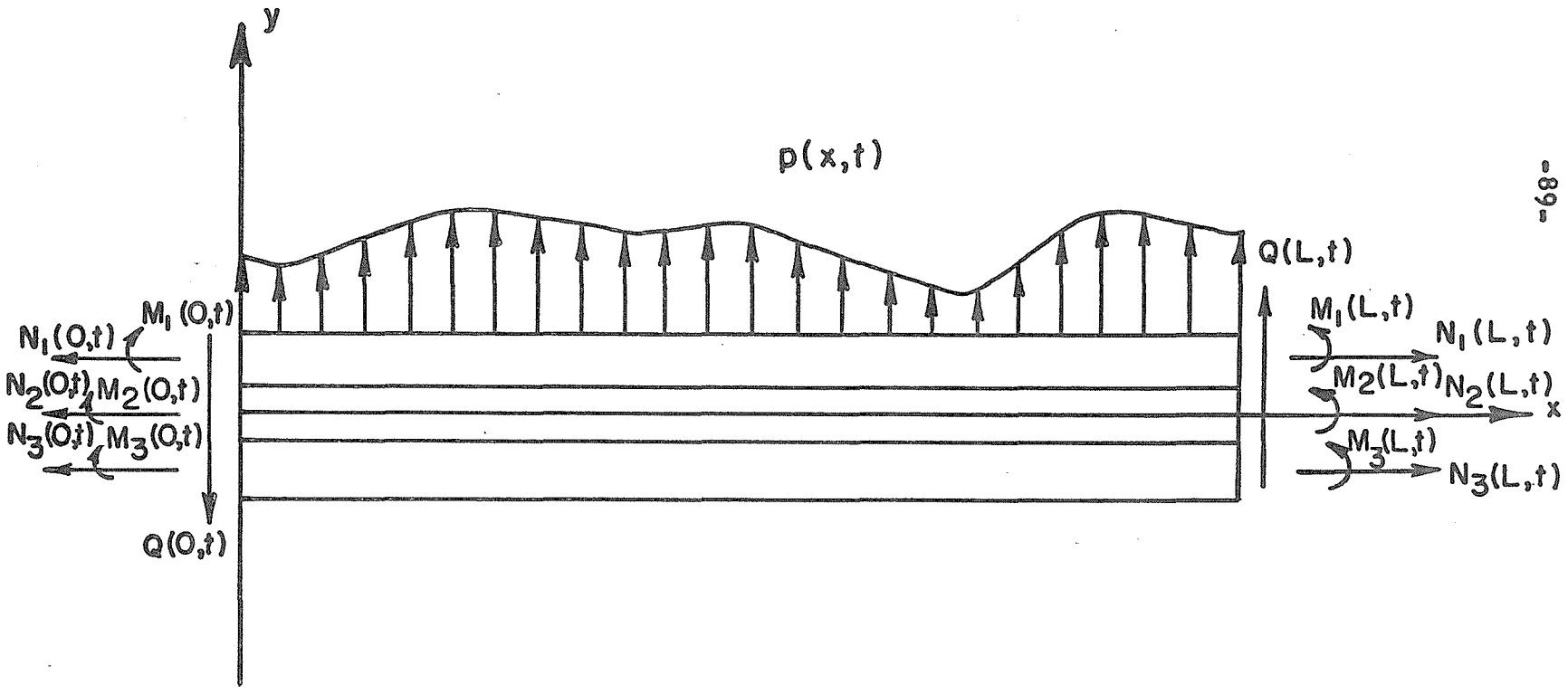

FIG. 3 NOMENCLATURE OF THE LOADING APPLIED TO THE BEAM

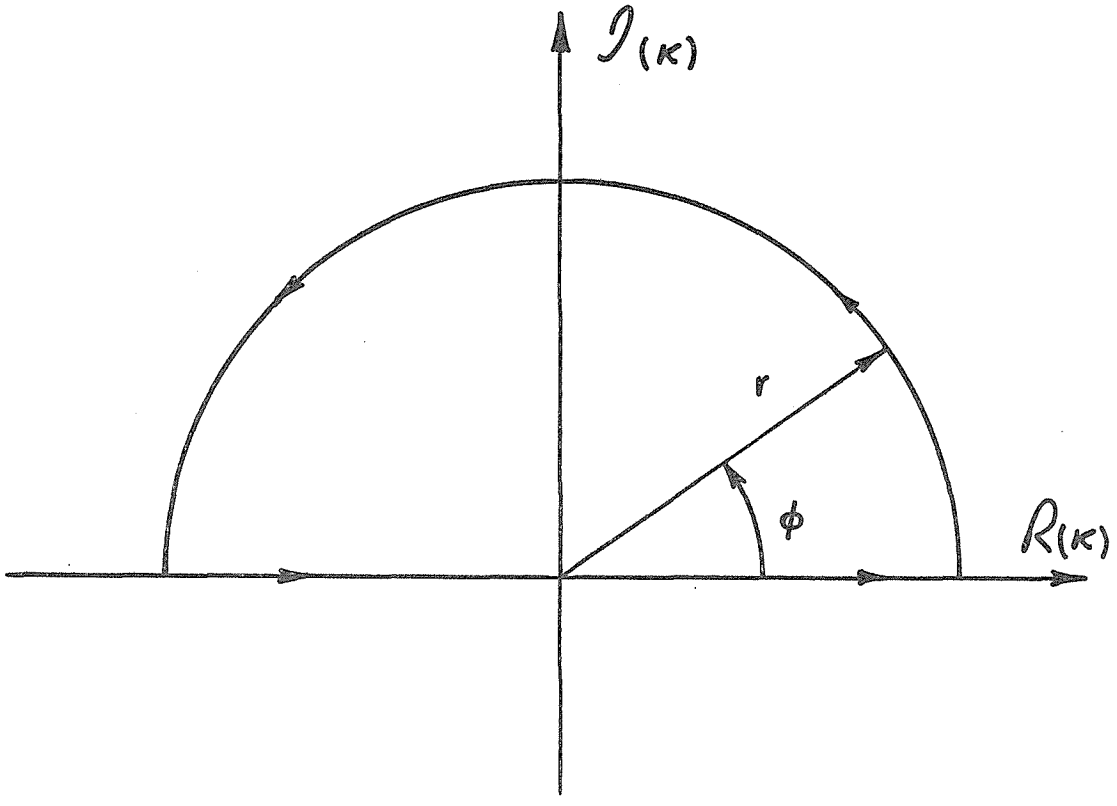

FIG. 4 CONTOUR C_r IN THE κ PLANE

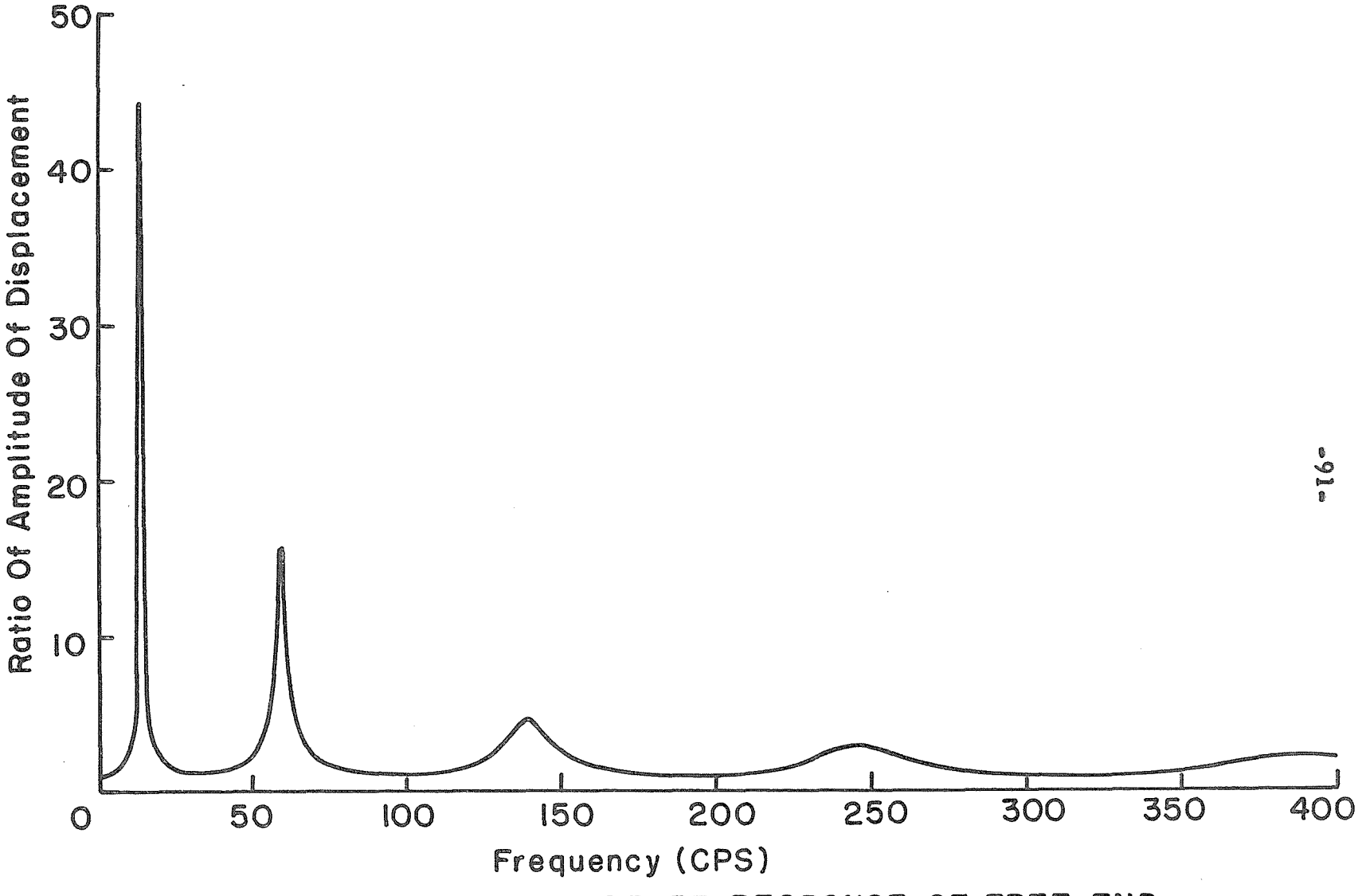

FIG. 5 THEORETICAL STEADY STATE RESPONSE OF FREE END

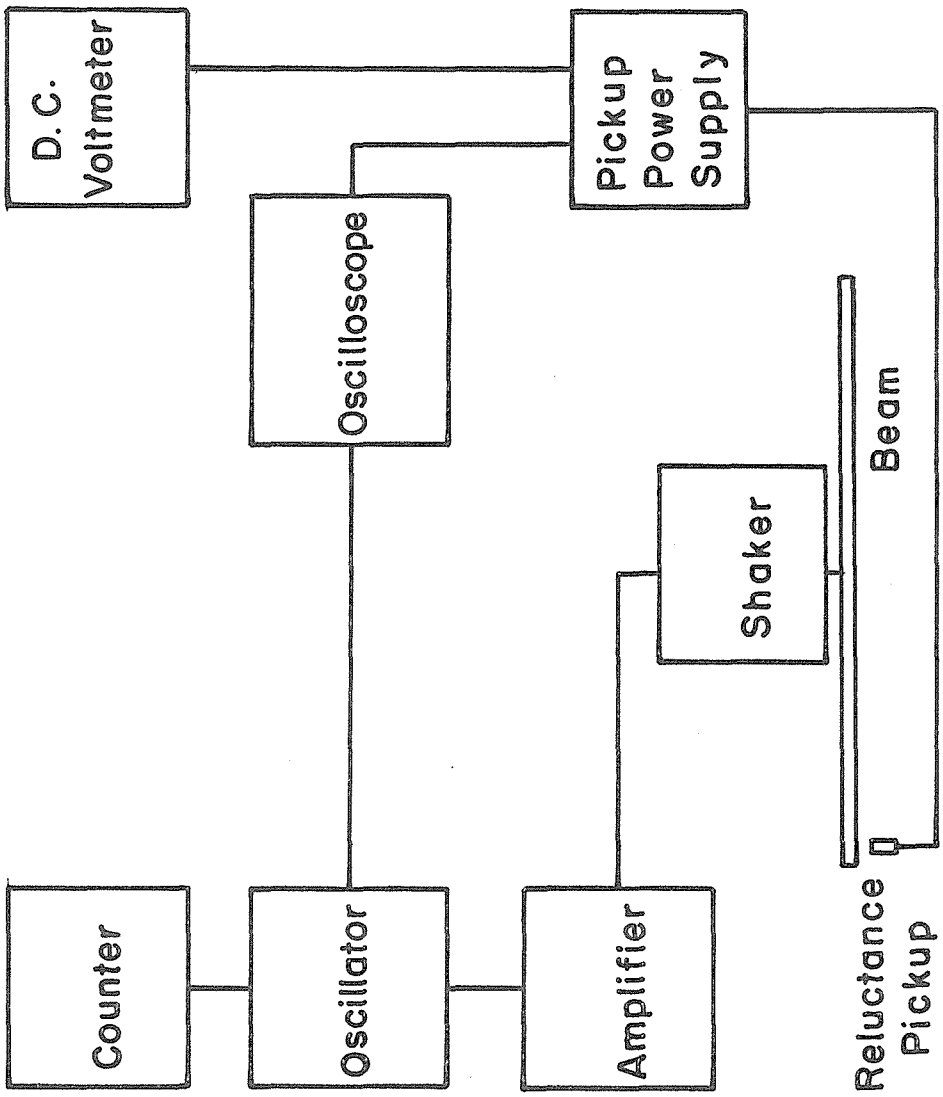

FIG. 6 EXPERIMENTAL SETUP

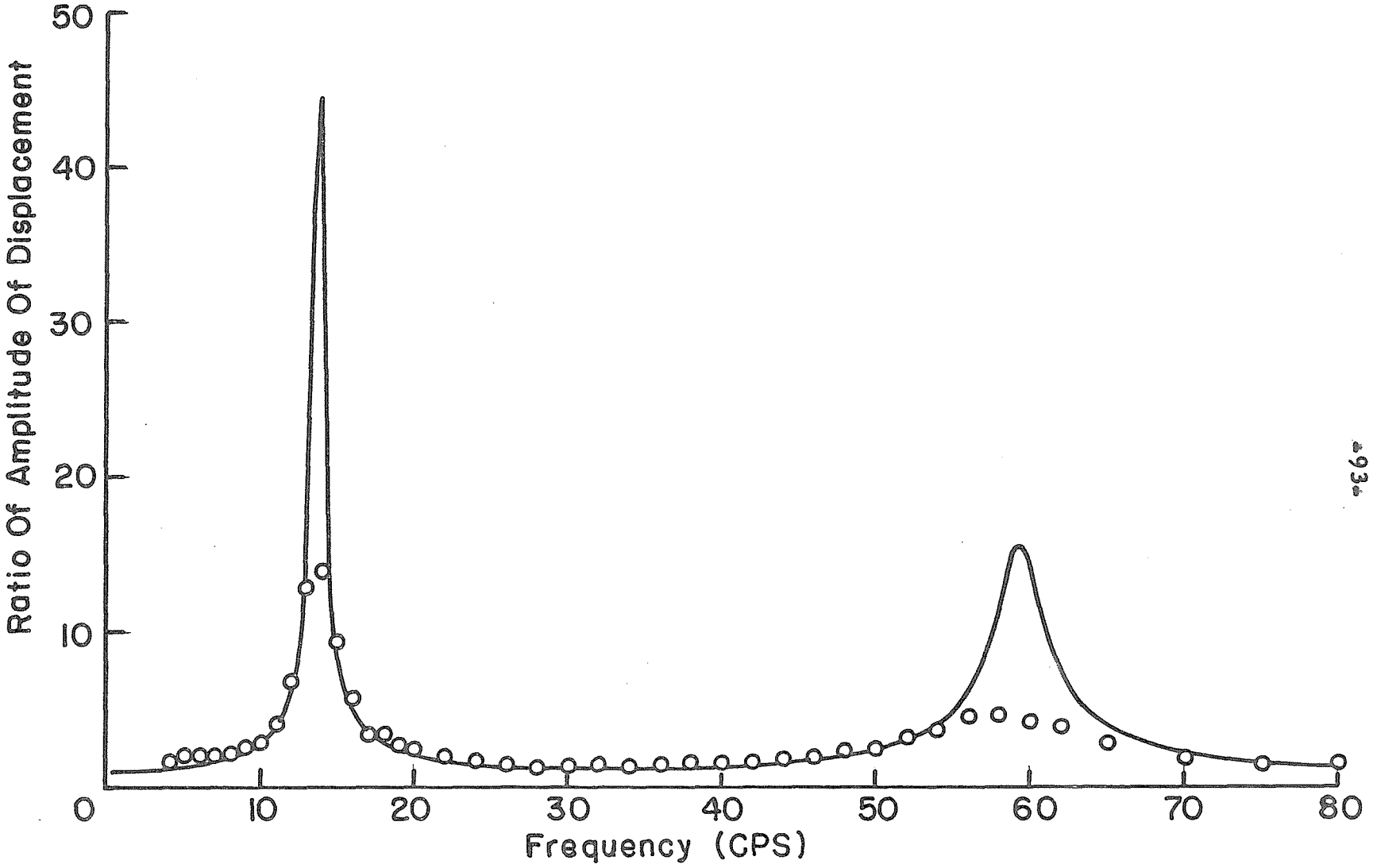

FIG. 7 EXPERIMENTAL RESULTS VS THEORETICAL RESPONSE CURVE, FREE END

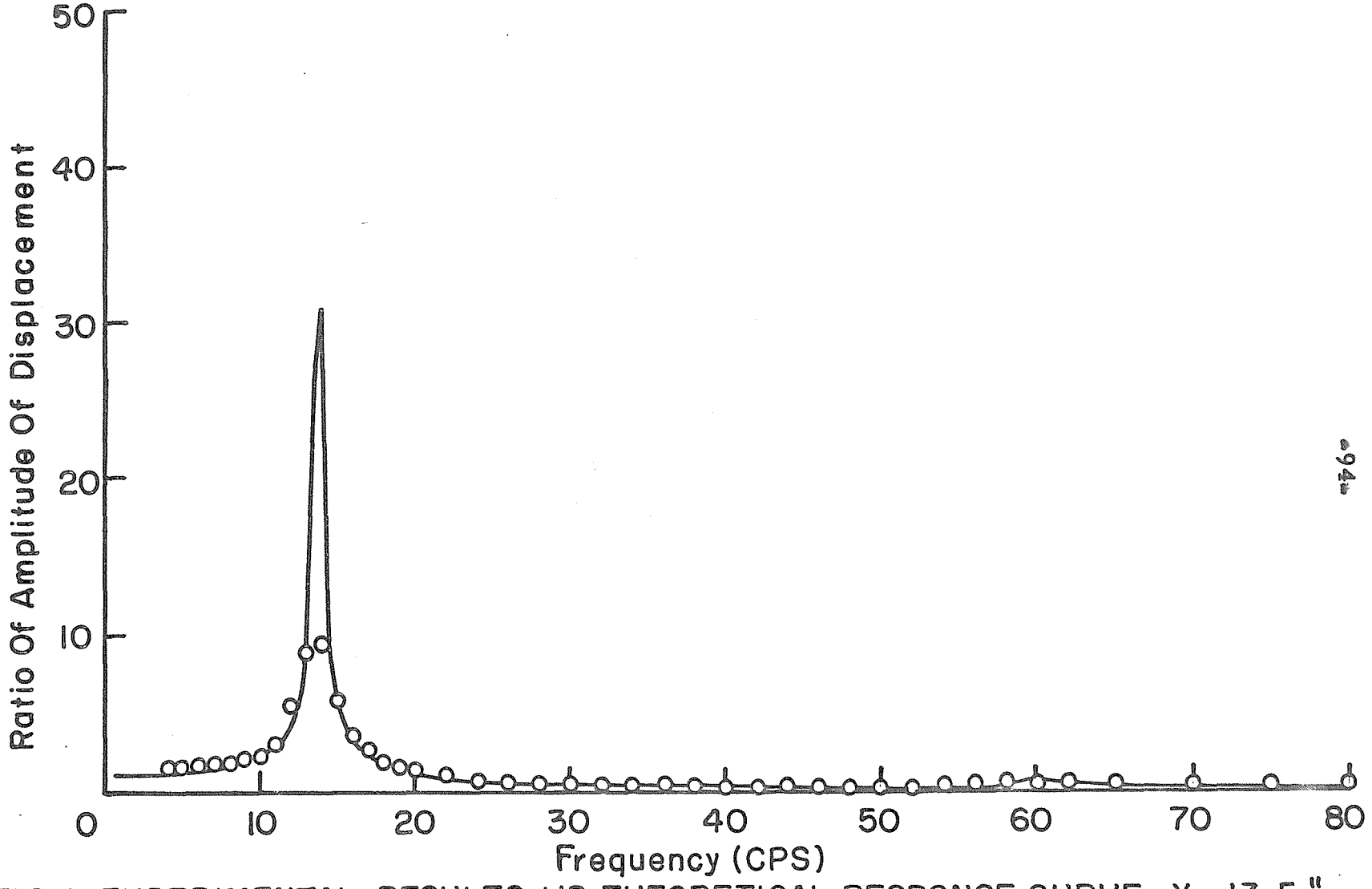

FIG. 8 EXPERIMENTAL RESULTS VS THEORETICAL RESPONSE CURVE, X = 13.5"

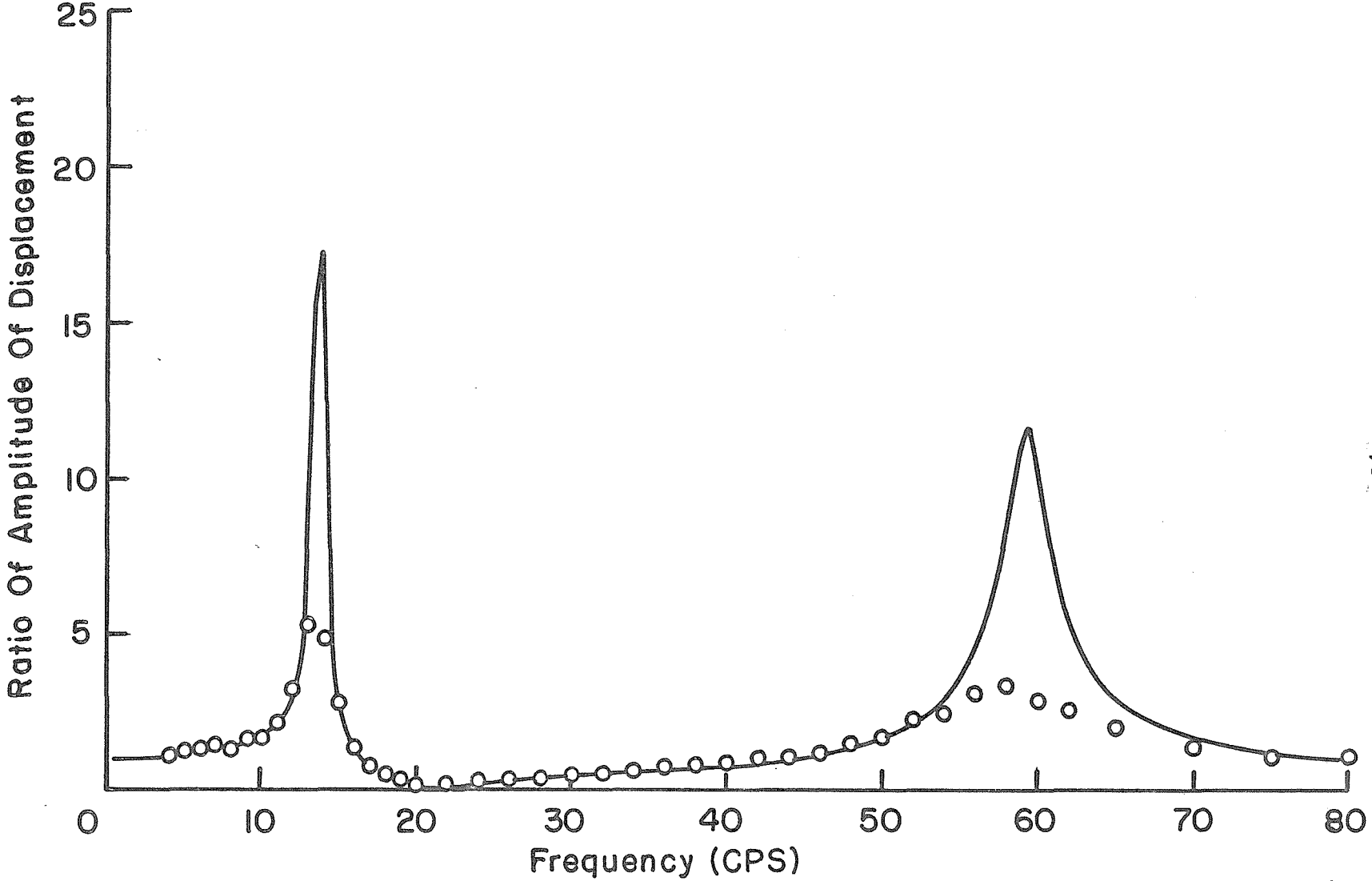

FIG. 9 EXPERIMENTAL RESULTS VS THEORETICAL RESPONSE CURVE, X= 9"

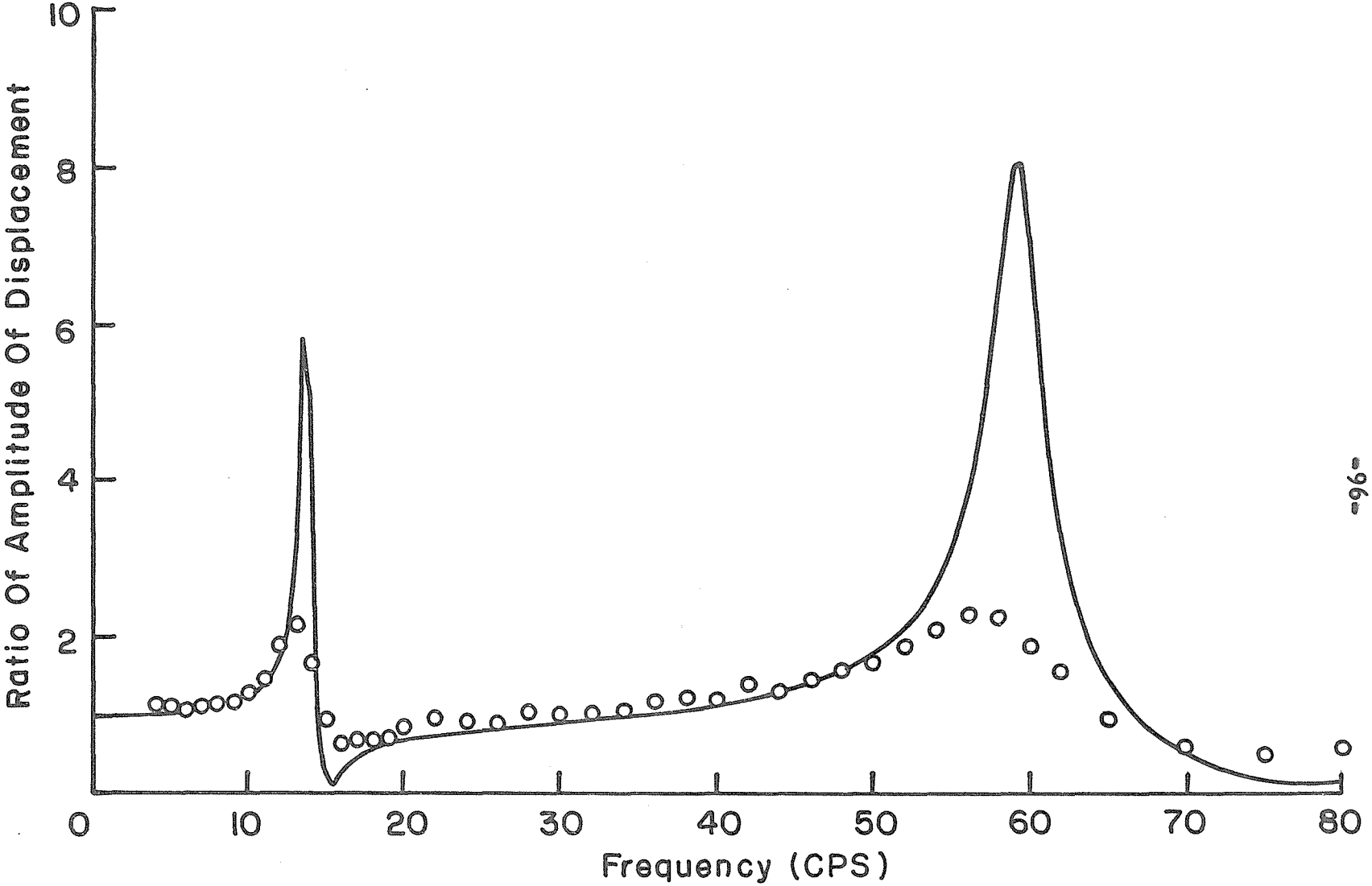

FIG. 10 EXPERIMENTAL RESULTS VS THEORETICAL RESPONSE CURVE, X=4.5"

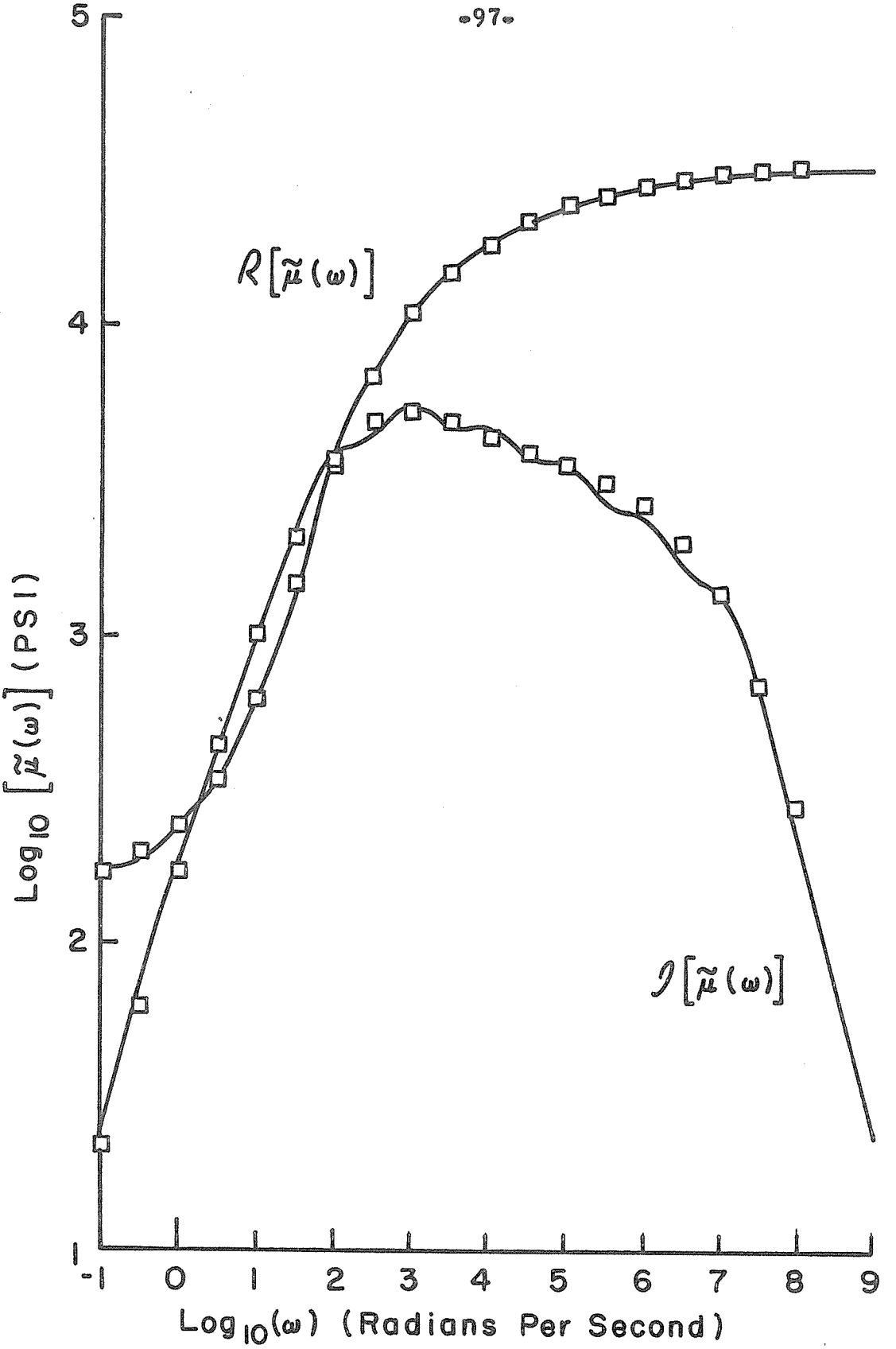

FIG. 11 COMPLEX SHEAR MODULUS REPRESENTATION OF TABLE 2

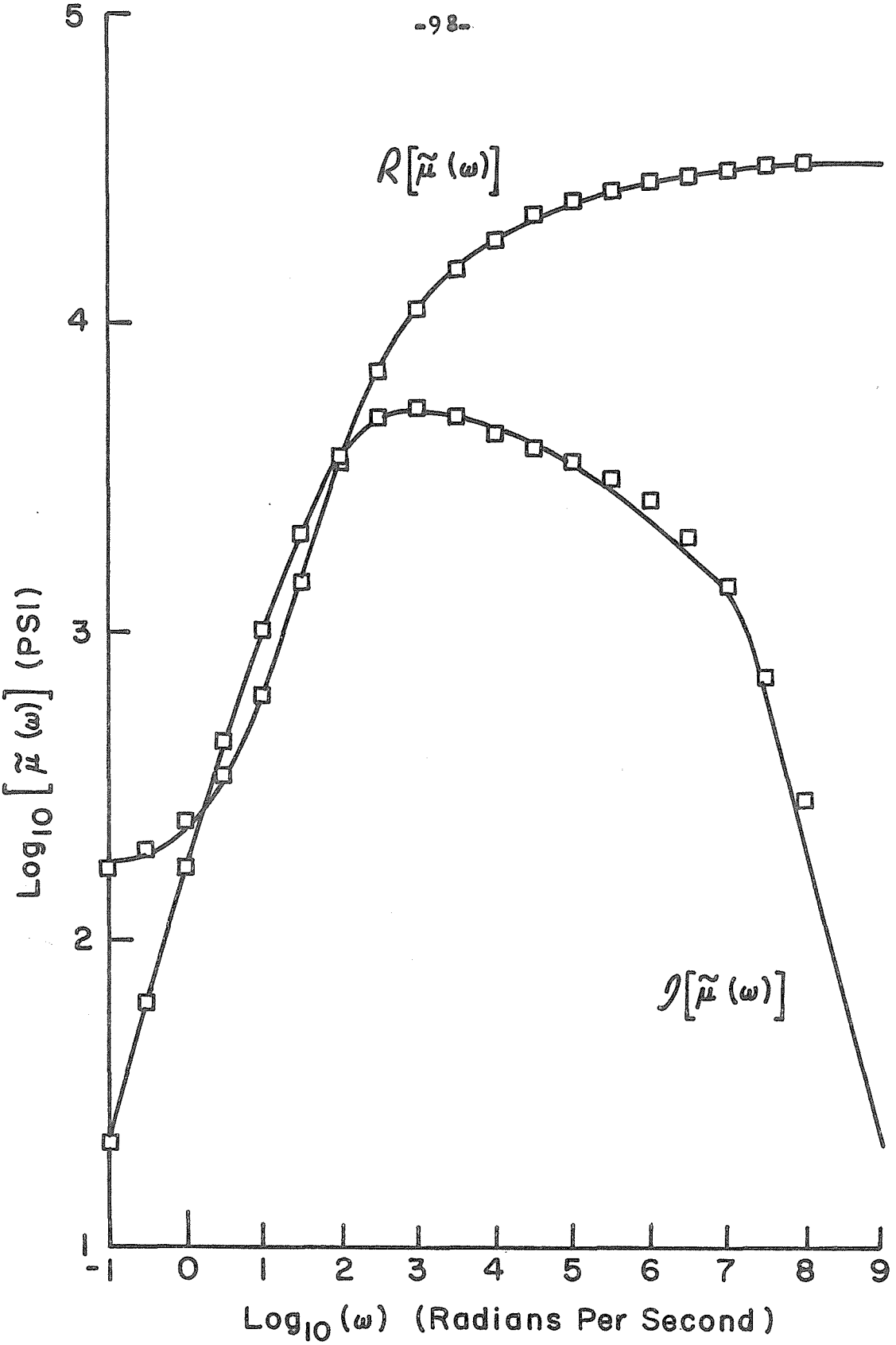

FIG. 12 COMPLEX SHEAR MODULUS REPRESENTATION OF TABLE 3

Table 1

Eigenvalues (radians per second)

n	ω_n Real	ω_n Imag	ν_{1n} x 10^{-3}	ν_{2n} x 10^{-4}	ν_{3n} x 10^{-5}	ν_{4n} x 10^{-6}	ν_{5n} x 10^{-7}	ν_{6n} x 10^{-8}	ν_{7n} x 10^{-9}	ν_{8n} x 10^{-10}
1	86.530	0.3558	2.3675	1.1254	0.7498	1.8779	2.8018	3.2187	3.5151	3.6998
2	372.95	9.0936	3.3436	2.0308	0.9001	1.9386	2.8284	3.2331	3.5228	3.7038
3	869.01	41.882	3.6089	2.8946	1.2246	2.0521	2.8783	3.2603	3.5373	3.7116
4	1540.2	88.512	3.7074	3.3383	1.6418	2.2037	2.9454	3.2973	3.5583	3.7222
5	2428.7	142.88	3.7441	3.5528	2.0496	2.3751	3.0231	3.3408	3.5810	3.7350
6	3529.2	195.80	3.7585	3.6649	2.3995	2.5498	3.1049	3.3876	3.6068	3.7489
7	4843.7	248.06	3.7763	3.7281	2.6821	2.7159	3.1859	3.4349	3.6332	3.7633
8	6367.1	302.18	3.7956	3.7667	2.9048	2.8668	3.2627	3.4808	3.6591	3.7775
9	8103.2	361.68	3.8136	3.7926	3.0789	2.9999	3.3334	3.5239	3.6838	3.7911
10	10052.	427.51	3.8294	3.8103	3.2155	3.1154	3.3972	3.5636	3.7067	3.8039
11	12218.	499.56	3.8433	3.8221	3.3234	3.2145	3.4539	3.5997	3.7278	3.8157
12	14601.	576.85	3.8554	3.8294	3.4095	3.2993	3.5040	3.6320	3.7469	3.8264

Table 2

Values of Parameters in the Expression for Complex Shear Modulus, (A. 2)

$\mu(0) = 32027.45$ PSI

n	τ_n (sec.)	μ_n (PSI)
1	10^{-7}	1951.87
2	10^{-6}	3278.64
3	10^{-5}	5027.02
4	10^{-4}	6602.71
5	10^{-3}	8583.79
6	10^{-2}	5742.27
7	10^{-1}	554.81
8	1	111.89

Table 3

Values of Parameters in the Expression for Complex Shear Modulus, (A. 2)

$\mu(0) = 31994.67$

n	τ_n (sec.)	μ_n (PSI)
1	1.0×10^{-7}	1601.74
2	3.162×10^{-7}	942.46
3	1.0×10^{-6}	1761.66
4	3.162×10^{-6}	1962.58
5	1.0×10^{-5}	2748.73
6	3.162×10^{-5}	2598.12
7	1.0×10^{-4}	3533.45
8	3.162×10^{-4}	3708.87
9	1.0×10^{-3}	4297.73
10	3.162×10^{-3}	4045.12
11	1.0×10^{-2}	3220.52
12	3.162×10^{-2}	832.42
13	1.0×10^{-1}	441.56
14	3.162×10^{-1}	45.99
15	1.0	73.81